A

| Structure | Nonproprietary name | Binding target | Affinity to FcRn $K_D$ (mM) | Half-life (days) cited from the literature | |
|---|---|---|---|---|---|
| Human antibody | Adalimumab | TNFα | 672 | 14.7-19.3 | Weisman et al., 2003 |
| Humanized antibody | Daclizumab | CD25 | 846 | 20 | Vincenti et al., 1998 |
| | Omalizumab | IgE | 1237 | 20 | Casale et al., 1997 |
| | Palivizumab | RSV F protein | 750 | 19.2 | Subramanian et al., 1998 |
| | Trastuzumab | HER2 | 773 | 2.7-10 | Tokuda et al., 1999 |
| Chimeric antibody | Infliximab | TNFα | 727 | 9.5 | Comillie et al., 2001 |
| | Rituximab | CD20 | 508 | 9.4 | Maloney et al., 1997 |
| Mouse antibody | Muromonab-CD3 | CD3 | ND | 0.75 | Hooks et al., 1991 |
| Fc-fusion protein | Abatacept | CD80/CD86 | 2633 | 13.1 | prescribing information |
| | Alefacept | CD2 | 2506 | 11.3 | prescribing information |
| | Etanercept | TNFα | 3612 | 4 | Lee et al., 2003 |

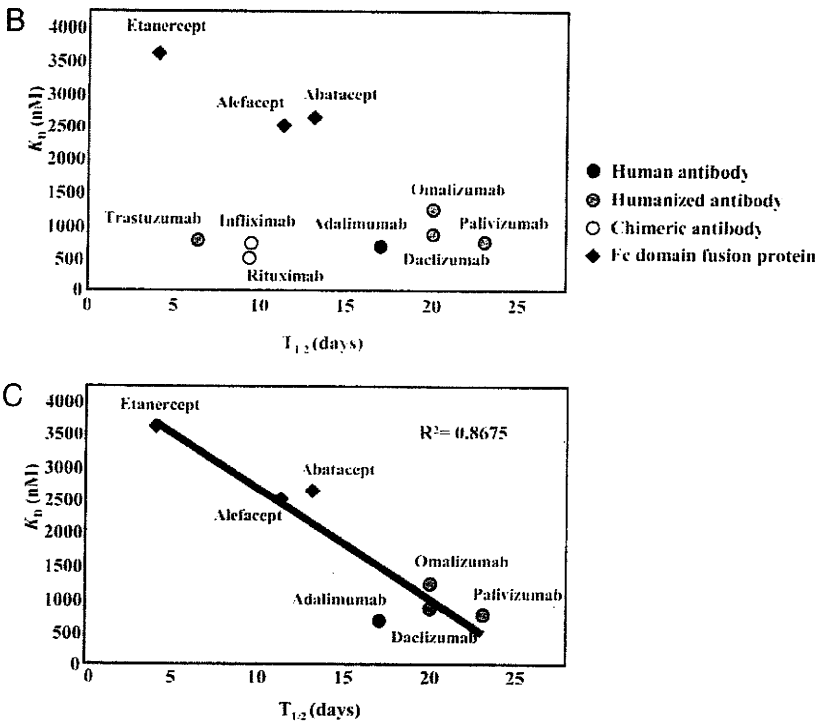


**FIGURE 3.** $K_D$ values of binding between Fc domain-containing therapeutic proteins and hFcRn and the correlation with their serum half-lives. *A*, The $K_D$ values obtained in our study and the half-lives in humans cited from the literature. The half-life values were obtained from the article reviewed by Lobo et al. (6) [adalimumab (17), daclizumab (18), etanercept (19), infliximab (20), muromonab-CD3 (21), omalizumab (22), palivizumab (23), rituximab (24), and trastuzumab (25)] or from the manufacturer prescribing information. *B*, The graphical presentation of the $K_D$ values and serum half-lives described in *A*. The means of half-lives are plotted on the *x*-axis, and the values of affinity to FcRn are on the *y*-axis. Filled rhombi, Fc domain fusion proteins; closed circle, human Ab; gray circles, humanized Abs; open circle, chimeric Abs. *C*, Regression line of the plots of seven therapeutic proteins. ND, not detected; $R^2$, coefficient of determination.

which exhibited no significant binding to human FcRn, the half-life of this Ab in humans is the shortest (0.75 d) among the therapeutic proteins examined in this study (21). These results also show the importance of the binding affinity to FcRn in determining the serum half-life. The correlation described above was also observed when other fractions of hFcRn described in Fig. 1 (peaks I and II) were used in SPR analyses (data not shown).

*The affinity between FcγRI and Fc domain-containing proteins*

Because the affinities of Fc fusion proteins (etanercept, alefacept, and abatacept) to FcRn were lower than those of mAbs, the FcRn-binding region (CH2-CH3 domain interface) of Fc-fusion proteins seems to be structurally different from that of mAbs. We also analyzed the affinity of these proteins to FcγRI to test whether the structural environment around the FcγRI-binding region (hinge proximal region of CH2) is different between Fc-fusion proteins and Abs. Because the regeneration procedure in the SPR assay inactivated FcγRI but not Fc domain-containing therapeutic proteins, therapeutic proteins were immobilized to CM5 biosensor chips, and FcγRI was used as an analyte. The sensorgrams of Fc-fusion proteins (abatacept, alefacept, and etanercept) and mAbs (adalimumab and infliximab) are shown in Fig. 4*A*. The data were analyzed with a 1:1 binding model. The $K_D$ values of the two Fc fusion proteins (alefacept and etanercept) and Abs (adalimumab and infliximab) were comparable (Fig. 4*B*). The $K_D$ values obtained in this study were similar to the data reported for IgG [reviewed by van de Winkel and Anderson (26)]. In contrast, abatacept had a lower affinity to FcγRI. In abatacept, a series of selected mutations those can alter the binding affinity to FcγR were introduced to reduce Fc-mediated cytotoxic effects (Fig. 5) (28, 29). Therefore, the data in Fig. 4 show that the change in the affinity of Fc domain to FcγRI, which is caused by amino acid substitutions, was detected in our experiments. These results suggest that the region interacting with FcγRI (i.e., the hinge proximal region of CH2) was not structurally different between Fc fusion proteins, except for abatacept, and Abs examined.

*The affinity between FcRn and Fc domains generated by papain treatment*

In Fig. 5, the amino acids sequences of abatacept, alefacept, etanercept, adalimumab, infliximab, and omalizuamb are aligned. The differences in the primary structure of the Fc regions were $Glu^{376}$ and $Met^{378}$ of etanercept, which are attributed to the IgG1 allotype, and $Ser^{162}$, $Ser^{165}$, and $Ser^{174}$ of abatacept, which are due

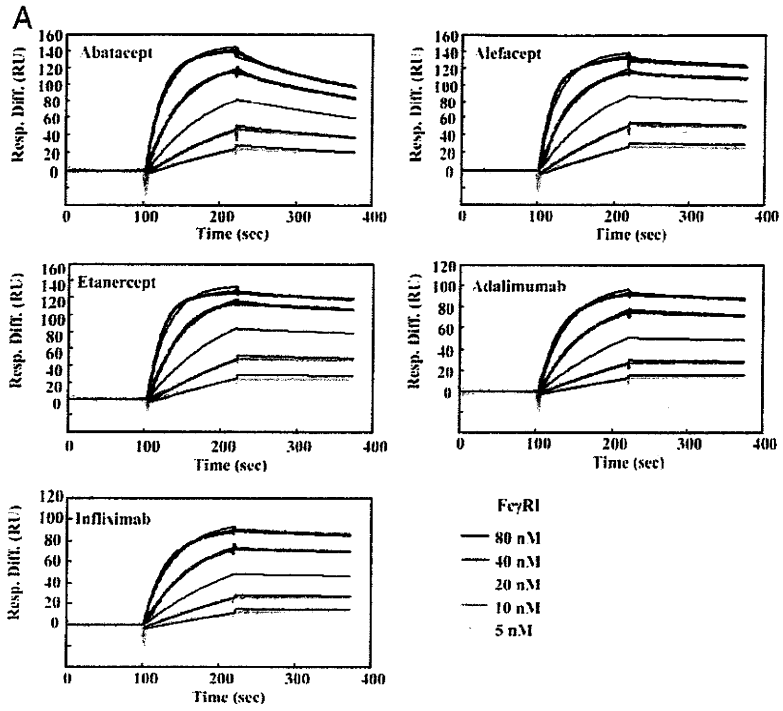


B

| | Affinity to FcγRI $K_D$ (nM) |
|---|---|
| Abatacept | 4.82 |
| Alefacept | 0.857 |
| Etanercept | 0.818 |
| Adalimumab | 0.779 |
| Infliximab | 0.763 |

**FIGURE 4.** The affinity of Fc-fusion proteins and Abs to FcγRI. The Fc-fusion proteins (abatacept, alefacept, and etanercept) and mAbs (adalimumab and infliximab) were immobilized onto CM5 biosensor chips. Recombinant protein of the extracellular domain of FcγRI was injected at concentrations of 5–80 nM and analyzed with a 1:1 binding model (*A*). The colored lines are the observed sensorgrams, and the black lines are fitting lines. Association phase, ~100–220 s; dissociation phase, ~220 s. *B*, The $K_D$ values calculated from the sensorgrams shown in *A*.

to the engineering for decreasing affinity to FcγR and improving protein production (28). To test the possibility that this limited structural difference or posttranscriptional modifications such as glycosylation can give rise to the difference in binding affinity to FcRn, we digested the Fc-fusion proteins or mAbs with papain and analyzed the affinity of their Fc domains to FcRn. The electrophoretic pattern of etanercept and adalimumab digested with papain is shown in Fig. 6*A*. Both etanercept and adalimumab were digested sufficiently for 24 h at 37°C under the conditions described in *Materials and Methods*, whereas digestion was not sufficient after incubating for 2 h. Therefore, the therapeutic proteins digested with papain for 24 h were used for the SPR analyses. The sensorgrams of etanercept (670 nM) and adalimumab (670 nM) were much different without incubation with papain, but they became almost identical after papain digestion (Fig. 6*B*). We measured the affinities to FcRn of five therapeutic proteins (etanercept, alefacept, adalimumab, infliximab, and omalizumab) digested with papain (Fig. 6*C*). Etanercept and alefacept are Fc-fusion proteins with low affinity to FcRn, and omalizumab is an Ab showing lower affinity to FcRn than other Abs. Because it was possible that the proteins were cleaved, in part, into smaller fragments than the Fc domain, the estimated $K_D$ values may have been larger than the actual values. However, it was very clear that the affinities of etanercept, alefacept, infliximab, and omalizumab were increased by papain treatment (Fig. 6*C*).

The affinity of Fc-fusion protein and Abs became comparable after papain digestion, showing that the differences in amino acid sequences or posttranslational modification of the Fc domain did not contribute to the difference in the binding affinity of these proteins to FcRn. It therefore seems likely that the receptor domain of the Fc-fusion protein makes a difference in the higher-order structure of the FcRn-binding region of Fc (i.e., CH2-CH3 interface) or interferes with the binding between Fc domain and FcRn by steric hindrance. Moreover, such a difference or interference seems to be involved in determining the affinity to FcRn for some kinds of Abs, because the $K_D$ values of infliximab and omalizumab were also increased significantly by papain treatment.

### *The affinity between FcRn and therapeutic proteins binding with target molecules*

On the basis of the results suggesting the possibility that another region besides the Fc domain influences the affinity of Fc domain-containing proteins to FcRn, we assumed that binding with the target molecule would also change the affinity to FcRn. Because adalimumab, infliximab, and etanercept bind to the same target molecule, TNF-α, we analyzed the effects of binding with TNF-α on the affinity of these therapeutic proteins to FcRn. First, 0–2680 nM TNF-α was added to 335 nM infliximab and incubated for at least 1 h. The resulting mixture was then injected into the flow cell, and the affinities to FcRn were analyzed. By adding TNF-α, the shape of the sensorgram was drastically altered (Fig. 7*A*). The Abs (adalimumab and infliximab) can maximally bind to two TNF-α trimers, whereas etanercept binds to one TNF-α trimer. When the relative concentrations of TNF-α are low, three molecules of the Ab can bind to each TNF-α trimer, and cross-linked TNF/Ab complexes are formed (30). To evaluate the affinity

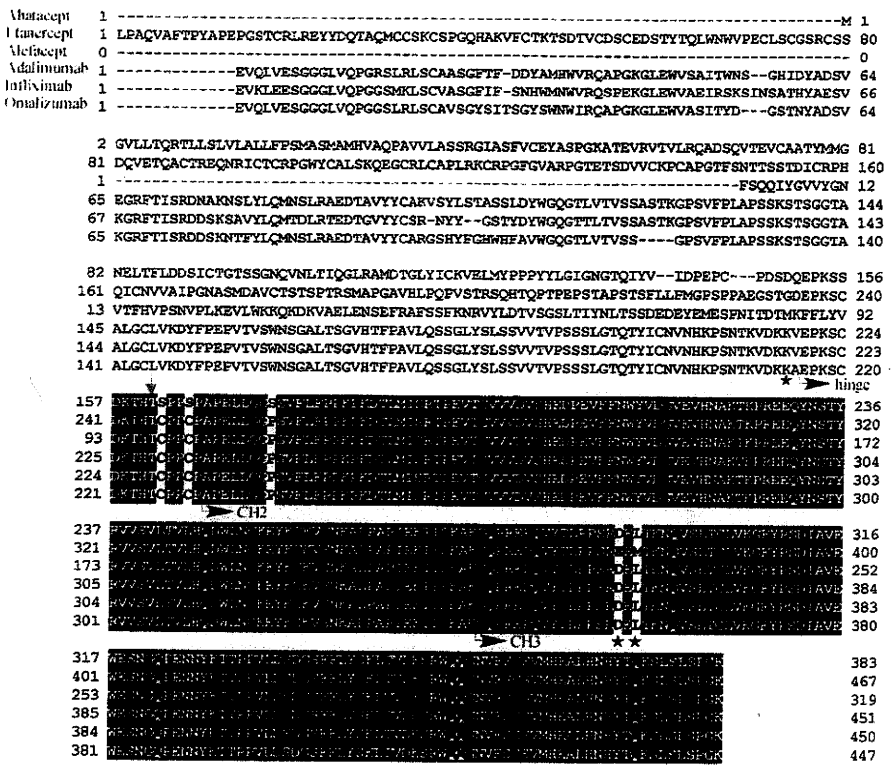


**FIGURE 5.** The amino acid sequences of abatacept, alefacept, etanercept, and H chains of adalimumab and infliximab. The amino acids marked with a star are different among allotypes of IgG1. The gray arrow is the cleavage site of IgG1 with papain (27). The amino acid sequences were obtained from the following links: abatacept, http://whqlibdoc.who.int/druginfo/18_2_2004_INN91.pdf; alefacept, http://whqlibdoc.who.int/druginfo/DRUG_INFO_14_4_2000_INN-84.pdf; etanercept, http://whqlibdoc.who.int/druginfo/DRUG_INFO_13_2_1999_INN-81.pdf; adalimumab, www.info.pmda.go.jp/shinyaku/g080405/10015900_22000AMX01598_A100_1.pdf; infliximab, www.info.pmda.go.jp/shinyaku/g020102/40031500_21400AMY00013_Q100_2.pdf; and omalizumab, www.drugbank.ca/drugs/DB00043.

between FcRn and TNF-α–binding proteins, excess TNF-α was added to adalimumab, infliximab, and etanercept (8-fold molar excess to 42–670 nM Abs and 4-fold to 168–2680 nM etanercept) to avoid forming nonuniform complexes. The sensorgrams were fitted by the bivalent analyte model (Fig. 7*B*). Although the fitted lines did not completely match the observed sensorgrams, the $K_D$ values of infliximab, adalimumab, and etanercept to FcRn were calculated to be 2057, 1321, and 4286 nM, respectively (Fig. 7*C*). The affinity of infliximab–TNF-α complex or adalimumab–TNF-α complex was lower than that of infliximab or adalimumab, respectively (Fig. 7*C*). These results suggest that at least for these anti–TNF-α Abs, binding with target molecules decreases the affinity to FcRn. They may also suggest that the anti–TNF-α Abs complexed with TNF-α will be degraded more rapidly than anti–TNF-α Abs free from TNF-α in vivo.

## Discussion

To our knowledge, this is the first article to elucidate the affinities of clinically used Fc domain-containing therapeutic proteins to FcRn in a comparative study. Because the affinities of these therapeutic proteins to FcRn were found to be highly correlated with the serum half-lives in humans, with the exception of infliximab, rituximab, and trastuzumab, the importance of FcRn in regulating the serum half-life of Fc domain-containing therapeutic proteins was suggested. The key observation was that the Fc-fusion proteins showed lower affinity to FcRn than Abs. These data provided us with one of the answers to the question of why the Fc-fusion proteins containing the Fc domain of human IgG1 exhibit a shorter half-life than human IgG1.

In the current study, we used the bivalent analyte model of BIAevaluation software. Most studies analyzing Fc-FcRn interactions have used the bivalent analyte model (15, 31) or the heterogeneous ligand model (7, 15, 31). Although the sensorgrams in our experiments were able to be fitted by both models, they were better fitted by the bivalent analyte model. Considering that two molecules of hFcRn bind to each IgG, resulting in a 2:1 binding stoichiometry (15), the bivalent analyte model seems to be suitable. It has been reported that the dual bivalent analyte model better fits the data of the FcRn-Fc interaction (32), although there are cases in which the bivalent analyte model does not work well. In the article about the dual bivalent analyte model, it was speculated that high-affinity and low-affinity types of FcRn existed on the surface of the BIAcore chip and that the low-affinity type receptor was probably an experimental artifact (32). Possibly because the content of the low-affinity type of FcRn on the chip is comparatively low in our immobilizing condition, the sensorgrams in our experiments might have been well-fitted by the bivalent analyte model.

Among the therapeutic proteins tested in this study, the Fc fusion proteins showed relatively lower affinities to FcRn (Figs. 2, 3), although the affinities to FcγRI are comparable to those of Abs (Fig. 4). Although the Fc domain binds to FcRn via the CH2-CH3 domain interface (33), the primary structures of the Fc domains of tested therapeutic proteins were almost the same, and cleavage of the Fc domains from Fab or the receptor region gave similar $K_D$ values to FcRn (Fig. 6). These results suggest that the receptor regions of Fc-fusion protein alter the conformation of the FcRn-binding region (CH2-CH3 domain interface), not of the FcγRI-binding region (hinge proximal region of CH2 domain), or cause steric hindrance on the CH2-CH3 domain interface. The influence of regions besides the Fc domain on FcRn-binding regions would also be the case for Abs, as shown in Fig. 7.

Our results presented in this study can provide valuable information regarding the molecular design of novel Fc domain-containing therapeutic proteins and demonstrate the usefulness of FcRn-binding analysis in the characterization of Fc domain-containing therapeutic proteins. In addition to the Fc fusion proteins used in this study, rilonacept, a Fc-fusion protein consisting of ligand-binding domains of the extracellular portions of the human IL-1 receptor component (IL-1RI) and IL-1 receptor accessory protein linked to the Fc portion of human IgG1, and romiplostim,

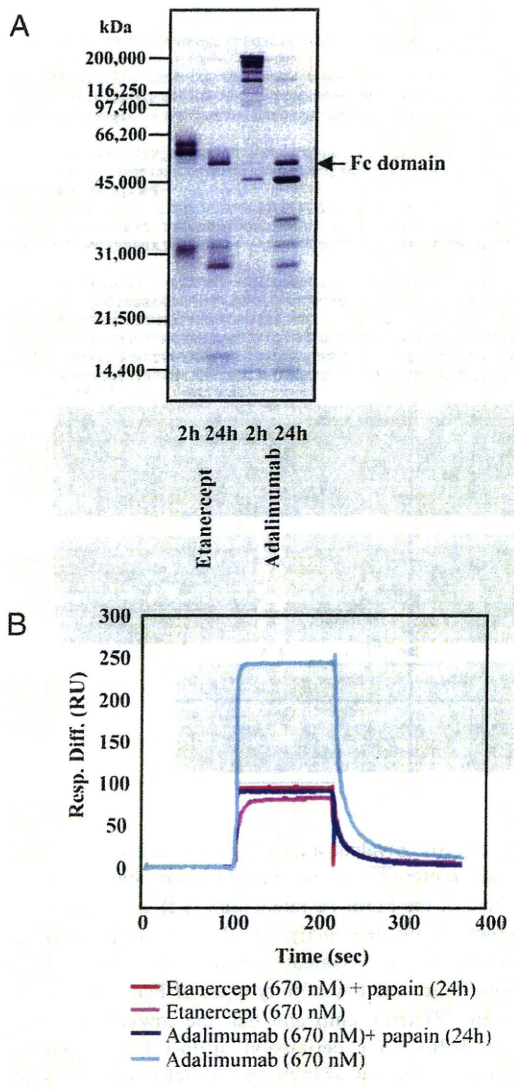


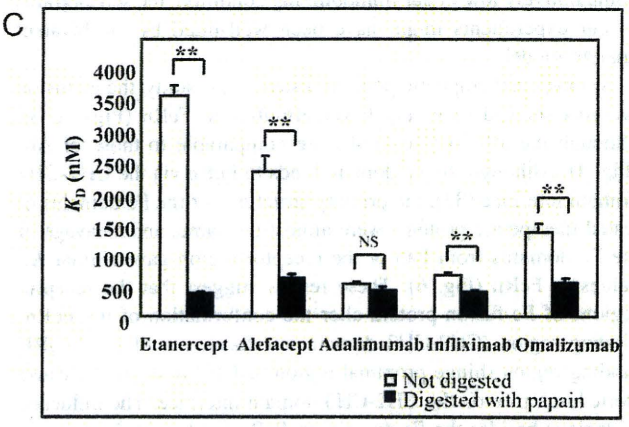


**FIGURE 6.** Effects of papain digestion on the affinities of Fc domain-containing therapeutic proteins to FcRn. *A*, The nonreduced SDS-PAGE of etanercept and adalimumab digested with papain for 2 and 24 h. *B*, The comparison between the sensorgrams of etanercept and adalimumab with or without papain digestion. *C*, Comparison of the affinity to FcRn among etanercept, alefacept, adalimumab, infliximab, and omalizumab, which were digested or not digested with papain. The $K_D$ values were calculated from the sensorgrams at the range of concentrations described as follows. The concentrations of papain-digested etanercept, papain-digested alefacept, adalimumab, papain-digested adalimumab, infliximab, papain-digested infliximab, and papain-digested omalizumab were 42–670 nM; those of etanercept and alefacept were 168–5360 nM, and those of omalizumab were 42–1340 nM. Each bar shows the average $K_D$ value + SD, which was calculated from three independent experiments. $^{**}p < 0.01$. NS, no significant difference according to Student *t* test.

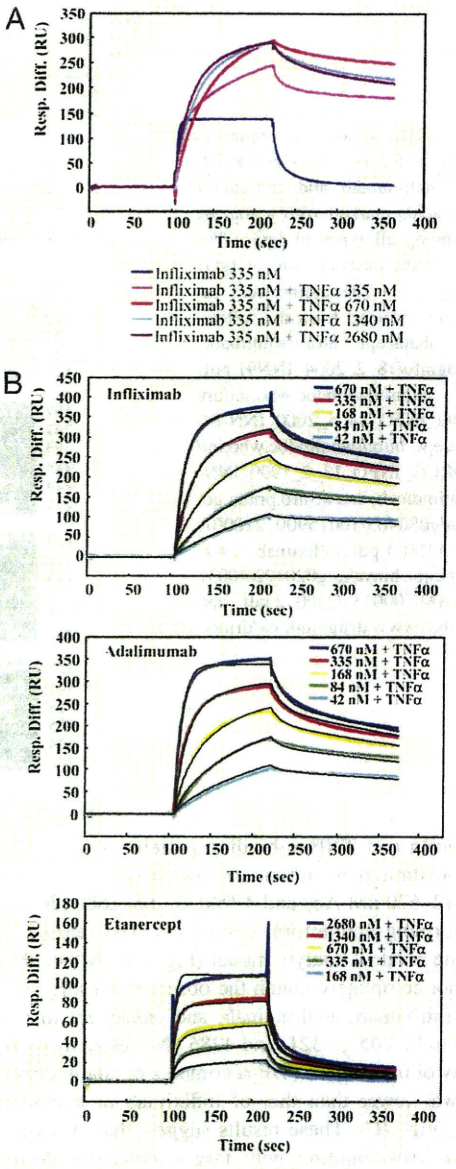


C

| | Affinity to FcRn $K_D$ (nM) | |
|---|---|---|
| | control | preincubate with TNFα |
| Etanercept | 3705 | 4286 |
| Adalimumab | 673 | 1321 |
| Infliximab | 751 | 2057 |

**FIGURE 7.** Effects of binding with the target molecules on the affinities of Fc domain-containing therapeutic proteins to FcRn. *A*, The sensorgrams of infliximab (335 nM) preincubated with TNF-α (0–2680 nM). *B*, The sensorgrams of infliximab (*upper panel*), adalimumab (*middle panel*), and etanercept (*lower panel*) preincubated with TNF-α (8-fold molar excess to 42–670 nM Abs and 4-fold to 168–2680 nM etanercept). The sensorgrams were fitted by the bivalent analyte model. *C*, The $K_D$ values calculated from the sensorgrams shown in *B*. The values of infliximab, adalimumab, and etanercept derived from the same series of experiments are also shown as controls.

a Fc-peptide fusion protein consisting of human IgG1 Fc domain linked at the C terminus to a peptide containing two thrombopoietin receptor-binding domains, were approved recently (34, 35). The

development of Fc-fusion proteins will receive further attention. Although the Fc domains are used with the intent of prolonging the half-lives of receptor proteins, the half-lives tend not to be fully prolonged to the level of IgG1. It remains unclear whether the receptor regions of Fc-fusion proteins alter the conformation of the CH2-CH3 domain interface or the regions cause steric hindrance on the binding site of FcRn; however, the molecular design of Fc-fusion proteins having a higher affinity to FcRn might be possible in either case.

Reflecting the increasing interest in the development of mAbs and related products, the newly revised guideline for such products was adopted by the European Medicines Agency in 2008 (www.emea.europa.eu/pdfs/human/bwp/15765307enfin.pdf). In the guidelines, it is mentioned that FcRn-binding activity should be provided, as appropriate, in product characterization. Because regions other than the Fc domain might affect the affinity of the protein to FcRn (Figs. 6, 7), the affinity to FcRn should be evaluated as an important quality attribute related to the pharmacokinetic profile, even if the protein has a native Fc domain of IgG1, especially in cases of Fc-fusion proteins. Meanwhile, because it was demonstrated that oxidation of two labile methionines, $Met^{252}$ and $Met^{428}$, in human IgG1 attenuates binding of the Ab to FcRn (36), alteration of the affinity to FcRn during the production process or storage will reflect structural changes of the protein, including Met oxidation, that will lead to shortening the serum half-life. In addition to IgG, albumin is also known to bind to FcRn in a pH-dependent manner and is protected from degradation (37, 38). The albumin-fusion proteins (e.g., albumin-IFN) or drugs having an albumin-binding moiety are being developed. FcRn-binding characteristics would also be important as a quality attribute of such products, which is related to the pharmacokinetic profile.

As mentioned above, the existence of several Abs having a short half-life and high affinity to FcRn suggested the involvement of other critical factor(s) in regulating the serum half-life of Abs such as trastuzumab, rituximab, or infliximab. Trastuzumab is a humanized Ab directed against human epidermal growth factor receptor 2 (HER2), which is expressed in some types of breast cancer cells. It has been reported that trastuzumab is taken up by HER2-expressing cells via HER2-mediated endocytosis (39, 40). Rituximab, a chimeric Ab directed against CD20, is also internalized in an Ag-mediated manner (41). Because the ligand-dependent internalization is followed by degradation of Abs, this property seems to be an important reason for the short half-life of trastuzumab and rituximab. It has been reported that, in general, the half-life of monoclonal IgG Abs increases depending on the degree of humanization in the order of murine < chimeric < humanized < human (6, 41, 42). Because infliximab and rituximab are chimeric Abs, the involvement of common factors influencing the half-life of chimeric Abs such as the presence of human anti-chimeric Ab would be another reason for the shorter half-life.

As shown in Fig. 7, the affinities of infliximab–TNF-α complex and adalimumab–TNF-α complex seemed to be lower than those of infliximab and adalimumab. If the affinity of therapeutic proteins/target molecules complexes to FcRn is lower than that of the free therapeutic proteins, the complexes will be degraded faster. Therefore, the half-lives of such therapeutic proteins seem to be shortened in the case that the target molecules are abundant in the bodies of patients. In contrast, if the affinity to FcRn of therapeutic proteins/target molecule complexes is higher than that of the free drugs, the complexes of drug and target molecules will have longer half-lives than free drugs. Because there are many factors affecting the elimination of Abs [reviewed by Tabrizi et al. (41)], further studies are necessary to elucidate the critical factors impacting the half-lives of Fc domain-containing proteins, in addition to the affinity to FcRn. Binding characteristics of the Fc domain-containing proteins or their complex with target molecules to FcγRs would be one of the important issues to be examined in regard to the impact on their elimination.

In conclusion, we showed the importance of the affinity to FcRn in determining the serum half-life of Fc domain-containing therapeutic proteins. Further investigation regarding the molecular structures that regulate the affinity of the engineered protein to FcRn will accelerate the development of therapeutic proteins with a desired half-life.

## Acknowledgments

We thank Dr. Pamela Bjorkman for the gift of the cell line expressing FcRn.

## Disclosures

The authors have no financial conflicts of interest.

## References

1. Morell, A., W. D. Terry, and T. A. Waldmann. 1970. Metabolic properties of IgG subclasses in man. *J. Clin. Invest.* 49: 673–680.
2. Simister, N. E., and K. E. Mostov. 1989. An Fc receptor structurally related to MHC class I antigens. *Nature* 337: 184–187.
3. Junghans, R. P., and C. L. Anderson. 1996. The protection receptor for IgG catabolism is the $\beta_2$-microglobulin-containing neonatal intestinal transport receptor. *Proc. Natl. Acad. Sci. USA* 93: 5512–5516.
4. Ghetie, V., S. Popov, J. Borvak, C. Radu, D. Matesoi, C. Medesan, R. J. Ober, and E. S. Ward. 1997. Increasing the serum persistence of an IgG fragment by random mutagenesis. *Nat. Biotechnol.* 15: 637–640.
5. Raghavan, M., V. R. Bonagura, S. L. Morrison, and P. J. Bjorkman. 1995. Analysis of the pH dependence of the neonatal Fc receptor/immunoglobulin G interaction using antibody and receptor variants. *Biochemistry* 34: 14649–14657.
6. Lobo, E. D., R. J. Hansen, and J. P. Balthasar. 2004. Antibody pharmacokinetics and pharmacodynamics. *J. Pharm. Sci.* 93: 2645–2668.
7. Datta-Mannan, A., D. R. Witcher, Y. Tang, J. Watkins, and V. J. Wroblewski. 2007. Monoclonal antibody clearance: impact of modulating the interaction of IgG with the neonatal Fc receptor. *J. Biol. Chem.* 282: 1709–1717.
8. Vaccaro, C., J. Zhou, R. J. Ober, and E. S. Ward. 2005. Engineering the Fc region of immunoglobulin G to modulate in vivo antibody levels. *Nat. Biotechnol.* 23: 1283–1288.
9. Hinton, P. R., J. M. Xiong, M. G. Johlfs, M. T. Tang, S. Keller, and N. Tsurushita. 2006. An engineered human IgG1 antibody with longer serum half-life. *J. Immunol.* 176: 346–356.
10. Dall'Acqua, W. F., P. A. Kiener, and H. Wu. 2006. Properties of human IgG1s engineered for enhanced binding to the neonatal Fc receptor (FcRn). *J. Biol. Chem.* 281: 23514–23524.
11. Petkova, S. B., S. Akilesh, T. J. Sproule, G. J. Christianson, H. Al Khabbaz, A. C. Brown, L. G. Presta, Y. G. Meng, and D. C. Roopenian. 2006. Enhanced half-life of genetically engineered human IgG1 antibodies in a humanized FcRn mouse model: potential application in humorally mediated autoimmune disease. *Int. Immunol.* 18: 1759–1769.
12. Yeung, Y. A., M. K. Leabman, J. S. Marvin, J. Qiu, C. W. Adams, S. Lien, M. A. Starovasnik, and H. B. Lowman. 2009. Engineering human IgG1 affinity to human neonatal Fc receptor: impact of affinity improvement on pharmacokinetics in primates. *J. Immunol.* 182: 7663–7671.
13. Nissim, A., and Y. Chernajovsky. 2008. Historical development of monoclonal antibody therapeutics. In *Therapeutic Antibodies (Handbook of Experimental Pharmacology)*, Vol. 181. Y. Chernajovsky and A. Nissim eds. Springer, New York, p. 3–18.
14. Reichert, J. M., C. J. Rosensweig, L. B. Faden, and M. C. Dewitz. 2005. Monoclonal antibody successes in the clinic. *Nat. Biotechnol.* 23: 1073–1078.
15. West, A. P., Jr., and P. J. Bjorkman. 2000. Crystal structure and immunoglobulin G binding properties of the human major histocompatibility complex-related Fc receptor. *Biochemistry* 39: 9698–9708.
16. Ellsworth, J. L., M. Maurer, B. Harder, N. Hamacher, M. Lantry, K. B. Lewis, S. Rene, K. Byrnes-Blake, S. Underwood, K. S. Waggie, et al. 2008. Targeting immune complex-mediated hypersensitivity with recombinant soluble human FcγRIA (CD64A). *J. Immunol.* 180: 580–589.
17. Weisman, M. H., L. W. Moreland, D. E. Furst, M. E. Weinblatt, E. C. Keystone, H. E. Paulus, L. S. Teoh, R. B. Velagapudi, P. A. Noertersheuser, G. R. Granneman, et al. 2003. Efficacy, pharmacokinetic, and safety assessment of adalimumab, a fully human anti-tumor necrosis factor-α monoclonal antibody, in adults with rheumatoid arthritis receiving concomitant methotrexate: a pilot study. *Clin. Ther.* 25: 1700–1721.
18. Vincenti, F., R. Kirkman, S. Light, G. Bumgardner, M. Pescovitz, P. Halloran, J. Neylan, A. Wilkinson, H. Ekberg, R. Gaston, et al. 1998. Interleukin-2-receptor blockade with daclizumab to prevent acute rejection in renal transplantation. *N. Engl. J. Med.* 338: 161–165.
19. Lee, H., H. C. Kimko, M. Rogge, D. Wang, I. Nestorov, and C. C. Peck. 2003. Population pharmacokinetic and pharmacodynamic modeling of etanercept using logistic regression analysis. *Clin. Pharmacol. Ther.* 73: 348–365.

20. Comillie, F., D. Shealy, G. D'Haens, K. Geboes, G. Van Assche, J. Ceuppens, C. Wagner, T. Schaible, S. E. Plevy, S. R. Targan, and P. Rutgeerts. 2001. Infliximab induces potent anti-inflammatory and local immunomodulatory activity but no systemic immune suppression in patients with Crohn's disease. *Aliment. Pharmacol. Ther.* 15: 463–473.
21. Hooks, M. A., C. S. Wade, and W. J. Millikan, Jr. 1991. Muromonab CD-3: a review of its pharmacology, pharmacokinetics, and clinical use in transplantation. *Pharmacotherapy* 11: 26–37.
22. Casale, T. B., I. L. Bernstein, W. W. Busse, C. F. LaForce, D. G. Tinkelman, R. R. Stoltz, R. J. Dockhorn, J. Reimann, J. Q. Su, R. B. Fick, Jr., and D. C. Adelman. 1997. Use of an anti-IgE humanized monoclonal antibody in ragweed-induced allergic rhinitis. *J. Allergy Clin. Immunol.* 100: 110–121.
23. Subramanian, K. N., L. E. Weisman, T. Rhodes, R. Ariagno, P. J. Sánchez, J. Steichen, L. B. Givner, T. L. Jennings, F. H. Top, Jr., D. Carlin, and E. Connor. 1998. Safety, tolerance and pharmacokinetics of a humanized monoclonal antibody to respiratory syncytial virus in premature infants and infants with bronchopulmonary dysplasia; MEDI-493 Study Group. *Pediatr. Infect. Dis. J.* 17: 110–115.
24. Maloney, D. G., A. J. Grillo-López, C. A. White, D. Bodkin, R. J. Schilder, J. A. Neidhart, N. Janakiraman, K. A. Foon, T. M. Liles, B. K. Dallaire, et al. 1997. IDEC-C2B8 (Rituximab) anti-CD20 monoclonal antibody therapy in patients with relapsed low-grade non-Hodgkin's lymphoma. *Blood* 90: 2188–2195.
25. Tokuda, Y., T. Watanabe, Y. Omuro, M. Ando, N. Katsumata, A. Okumura, M. Ohta, H. Fujii, Y. Sasaki, T. Niwa, and T. Tajima. 1999. Dose escalation and pharmacokinetic study of a humanized anti-HER2 monoclonal antibody in patients with HER2/neu-overexpressing metastatic breast cancer. *Br. J. Cancer* 81: 1419–1425.
26. van de Winkel, J. G., and C. L. Anderson. 1991. Biology of human immunoglobulin G Fc receptors. *J. Leukoc. Biol.* 49: 511–524.
27. Wenig, K., L. Chatwell, U. von Pawel-Rammingen, L. Björck, R. Huber, and P. Sondermann. 2004. Structure of the streptococcal endopeptidase IdeS, a cysteine proteinase with strict specificity for IgG. *Proc. Natl. Acad. Sci. USA* 101: 17371–17376.
28. Davis, P. M., R. Abraham, L. Xu, S. G. Nadler, and S. J. Suchard. 2007. Abatacept binds to the Fc receptor CD64 but does not mediate complement-dependent cytotoxicity or antibody-dependent cellular cytotoxicity. *J. Rheumatol.* 34: 2204–2210.
29. Presta, L. G. 2008. Molecular engineering and design of therapeutic antibodies. *Curr. Opin. Immunol.* 20: 460–470.
30. Scallon, B., A. Cai, N. Solowski, A. Rosenberg, X. Y. Song, D. Shealy, and C. Wagner. 2002. Binding and functional comparisons of two types of tumor necrosis factor antagonists. *J. Pharmacol. Exp. Ther.* 301: 418–426.
31. Martin, W. L., and P. J. Bjorkman. 1999. Characterization of the 2:1 complex between the class I MHC-related Fc receptor and its Fc ligand in solution. *Biochemistry* 38: 12639–12647.
32. Gurbaxani, B. M., and S. L. Morrison. 2006. Development of new models for the analysis of Fc-FcRn interactions. *Mol. Immunol.* 43: 1379–1389.
33. Martin, W. L., A. P. West, Jr., L. Gan, and P. J. Bjorkman. 2001. Crystal structure at 2.8 A of an FcRn/heterodimeric Fc complex: mechanism of pH-dependent binding. *Mol. Cell* 7: 867–877.
34. Osborne, R. 2009. Fresh from the biologic pipeline. *Nat. Biotechnol.* 27: 222–225.
35. Cines, D. B., U. Yasothan, and P. Kirkpatrick. 2008. Romiplostim. *Nat. Rev. Drug Discov.* 7: 887–888.
36. Pan, H., K. Chen, L. Chu, F. Kinderman, I. Apostol, and G. Huang. 2009. Methionine oxidation in human IgG2 Fc decreases binding affinities to protein A and FcRn. *Protein Sci.* 18: 424–433.
37. Chaudhury, C., S. Mehnaz, J. M. Robinson, W. L. Hayton, D. K. Pearl, D. C. Roopenian, and C. L. Anderson. 2003. The major histocompatibility complex-related Fc receptor for IgG (FcRn) binds albumin and prolongs its lifespan. *J. Exp. Med.* 197: 315–322.
38. Chaudhury, C., C. L. Brooks, D. C. Carter, J. M. Robinson, and C. L. Anderson. 2006. Albumin binding to FcRn: distinct from the FcRn-IgG interaction. *Biochemistry* 45: 4983–4990.
39. Steinhauser, I., B. Spänkuch, K. Strebhardt, and K. Langer. 2006. Trastuzumab-modified nanoparticles: optimisation of preparation and uptake in cancer cells. *Biomaterials* 27: 4975–4983.
40. Wuang, S. C., K. G. Neoh, E. T. Kang, D. W. Pack, and D. E. Leckband. 2008. HER-2-mediated endocytosis of magnetic nanospheres and the implications in cell targeting and particle magnetization. *Biomaterials* 29: 2270–2279.
41. Tabrizi, M. A., C. M. Tseng, and L. K. Roskos. 2006. Elimination mechanisms of therapeutic monoclonal antibodies. *Drug Discov. Today* 11: 81–88.
42. Kuester, K., and C. Kloft. 2006. Pharmacokinetics of monoclonal antibodies. In *Pharmacokinetics and Pharmacodynamics of Biotech Drugs*. B. Meibohm, ed. Wiley-VCH Verlag, Weinheim, Germany, p. 45–91.

—Regular Articles—

# 日本薬局方医薬品各条ヘパリンナトリウム純度試験へのキャピラリー電気泳動法の適用について

柊 直孝,[a] 木下充弘,[a] 川崎ナナ,[b] 山口照英,[b] 早川堯夫,[c] 掛樋一晃*,[a]

# Capillary Electrophoresis Analysis of Contaminants in Heparin Sodium for the Japanese Pharmacopoeia Purity Test

Naotaka KAKOI,[a] Mitsuhiro KINOSHITA,[a] Nana KAWASAKI,[b] Teruhide YAMAGUCHI,[b] Takao HAYAKAWA,[c] and Kazuaki KAKEHI*,[a]

[a]*Department of Biopharmaco Informatics, School of Pharmacy, Kinki University, 3-4-1 Kowakae, Higashi-Osaka 577-8502, Japan,*[b]*Division on Biological Chemistry & Biologicals, National Institute of Health Sciences, 1-18-1 Kamiyoga, Setagaya-ku, Tokyo 158-8501, Japan, and* [c]*Pharmaceutical Research and Technology, Kinki University, 3-4-1 Kowakae, Higashi-Osaka 577-8502, Japan*

(Received June 6, 2009; Accepted July 6, 2009; Published online July 7, 2009)

Heparin is widely used as an anticoagulant for the treatment and prevention of thrombotic disorders. Recently, hundreds of cases of anaphylactic reaction as adverse effects were reported by the presence of contaminating oversulfated chondroitin sulfate (OSCS) in some heparin preparations. In addition, these heparin preparations often contaminated dermatan sulfate (DS). Unfortunately, the Japanese Pharmacopoeia (JP) does not include appropriate purity tests. In the present paper, we show that capillary electrophoresis (CE) is a powerful tool for the analysis of OSCS and DS in heparin preparations. CE method shows high resolution and good quantification of OSCS in heparin preparations. This method (OSCS method) was evaluated for accuracy (93.7 %), repeatability (R.S.D.=2.11), linearity ($R^2$=0.9996), detection limit (0.1% OSCS) and specificity. In contrast, DS was not able to be detected in high sensitivity by OSCS method. However, a modified CE method (DS method) using the buffer at lower pHs showed good parameters for accuracy (88.1%), repeatability (R.S.D.=1.99), linearity ($R^2$=0.9998), detection limit (0.25% DS) and specificity. In conclusion, CE will be an alternative to the NMR method which is being adopted for purification test of heparin sodium in the present version of JP.

**Key words**——capillary electrophoresis; heparin sodium; oversulfated chondroitin sulfate; dermatan sulfate

## 緒 言

ヘパリンナトリウムは，ウロン酸（L-イズロン酸またはD-グルクロン酸）とD-グルコサミンの2糖単位の繰り返し構造に，2糖あたり平均2-3個の硫酸基を持つ構造からなる硫酸化グリコサミノグリカンのナトリウム塩である［Fig. 1(a)］．ヘパリンナトリウムは，アンチトロンビンⅢと特異的に結合することにより，第Ⅱa因子や第Xa因子などの血液凝固因子を阻害し血液凝固防止作用を示す.[1,2] そのため，血液透析などの体外循環装置使用時の血液凝固防止剤として世界中で汎用されるなど，臨床上極めて重要な医薬品であり，第15改正日本薬局方に収載されている．また，低分子量ヘパリン製剤の原料としても使用されている.[3]

2007年12月米国において，Baxter社製ヘパリンナトリウム製剤の静脈内急速大量投与を受けた患者に，血圧低下や頻脈等を伴うアレルギー反応が頻発し，80名以上の死亡例が報告された.[4] これまでヘパリン関連製剤に関して，血小板減少症などの副作用が知られていたが，今回発生した副作用はこれまでの報告例とは明らかに異なるものであった．さらに，ドイツでも別メーカーが製造したヘパリンナトリウム製剤の投与を受けた患者に同様のアレルギー反応がみられたことから国際的な問題へと発展した．2008年3月，米国食品医薬品局（FDA）は有害事象が多発したロットにヘパリン様物質が混入してい

[a]近畿大学薬学部生物情報薬学研究室，[b]国立医薬品食品衛生研究所生物薬品部，[c]近畿大学薬学総合研究所
*e-mail: k_kakehi@phar.kindai.ac.jp

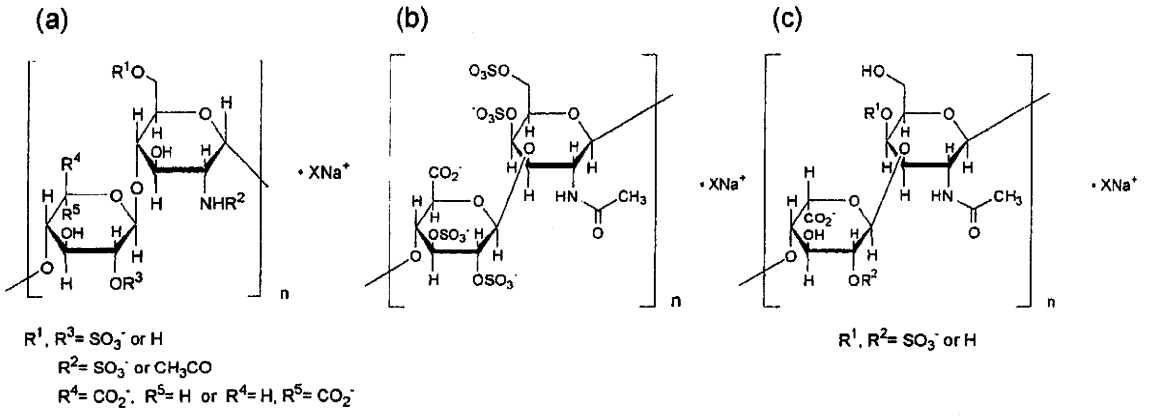


Fig. 1. Structures of the Disaccharide Unit of Glycosaminoglycans Tested in the Present Study
(a) Heparin sodium, (b) oversulfated chondroitin sulfate (OSCS) and (c) dermatan sulfate (DS).

ることを発表し,[5] のちに Guerrini らによる 2 次元 NMR などを用いる構造解析によって，このヘパリン様物質は過硫酸化コンドロイチン硫酸（oversulfated chondroitin sulfate; OSCS）であることが明らかにされた.[6] 通常，天然に存在するコンドロイチン硫酸は，D-グルクロン酸と N-アセチルガラクトサミンの 2 糖単位に，硫酸基が 1—3 個結合している．しかし，問題のヘパリンナトリウム製剤に混入していた OSCS は，コンドロイチン硫酸中のすべての水酸基が硫酸化され，2 糖単位中に硫酸基が 4 個結合した構造であった [Fig. 1 (b)]．また，有害事象を引き起こしたヘパリンナトリウム中には，OSCS に加えて，同じ硫酸化グリコサミノグリカン類の一種であるデルマタン硫酸（dermatan sulfate; DS，別名：コンドロイチン硫酸 B) [Fig. 1 (c)] も，従来の製品よりも多量に含まれていることが明らかにされた.

FDA は，有害事象の原因物質として OSCS を特定したことを発表するとほぼ同時に，$^1$H- 核磁気共鳴スペクトル測定法（$^1$H-NMR）とキャピラリー電気泳動法を用いる OSCS の検出法をインターネット上に公開した.[7,8] $^1$H-NMR は，ヘパリンナトリウム中の N-アセチルグルコサミンの N-アセチル基と，OSCS 中の N-アセチルガラクトサミンの N-アセチル基の化学シフトが異なることを利用する検出法である．また，キャピラリー電気泳動法はヘパリンナトリウムと OSCS の硫酸基の結合数の違いを利用する分離分析をもとにする検出法である．さらに，陰イオン交換カラムを用いる HPLC 法や，単糖組成分析法，Inhibition of Taq polymerase 法などによる OSCS 検出法が次々に報告された.[9-11] 各国は，これらの検出法を用いてヘパリンナトリウム製剤の分析を行うとともに，OSCS の存在が確認されたヘパリンナトリウム製剤の回収を行う等の対応をとった．わが国でも，問題のヘパリンナトリウム製剤と同じ SPL 社の原薬を使用した国内 3 社が予防的措置として自主回収を行った．そのため，世界的にヘパリン関連医薬品の供給不足への懸念が広がり，ヘパリンナトリウム製剤の安定供給のために，ヘパリンナトリウム原料中の OSCS 及び DS の試験法の整備が緊急課題となった.

問題発生時，第 15 改正日本薬局方医薬品各条ヘパリンナトリウムの項には，バリウムやタンパク質などに関する純度試験が規定されていたが，記載されている試験法では OSCS 混入の有無を評価することができない．そこでわが国においても FDA が公開した試験法を参考に，$^1$H-NMR 及びキャピラリー電気泳動法による日本薬局方への適用を目的とした分析法バリデーションが行われた.[12,13] その結果，官報号外第 166 号（平成 20 年 7 月 31 日）において，「ヘパリンナトリウムに関する日本薬局方の一部改正に伴う取り扱いについて」として，$^1$H-NMR を用いる OSCS の限度試験が導入されることとなった．なお，今回の改正では，キャピラリー電気泳動法による試験の導入は見送られた．その理由として，FDA が公開したキャピラリー電気泳動法の条件は，ヘパリンナトリウムと OSCS のピークの分離が不十分であり，OSCS 検出の特異性や検出感度に問題があったためである.[13] しかし，キャピラリー電気泳動法はルーチン分析に適した分

析法であり，またヘパリンナトリウム中のOSCSやDSを検出できる数少ない分析法の1つであることなどからその価値は高く，米国薬局方ではヘパリンナトリウム確認試験に，また，欧州薬局方ではヘパリンナトリウムの製造部分の試験法に採用されている．

本研究では，ヘパリンナトリウム製剤の品質・安全性確保を目的として，キャピラリー電気泳動法による試験法を確立すると共に，分析法バリデーションを実施し，日本薬局方医薬品各条ヘパリンナトリウム純度試験としての適用可能性を検証した．

## 実験方法

**1. 試料及び試薬** ヘパリンナトリウムは日本薬局方ヘパリンナトリウム標準品を使用した．OSCSは日本薬局方過硫酸化コンドロイチン硫酸標準品を使用した．なお，分析条件の検討には，生化学用ヘパリン（Sigma社製，ブタ腸粘膜由来）を使用した．DS（ブタ皮膚由来）は生化学工業㈱から購入した．OSCSを含有するヘパリンナトリウム製剤原料は日本バルク薬品㈱より供与を受けた．その他の試薬は特級品，あるいはHPLCグレードを使用した．本試験に用いた水は，MILLIPORE Direct-Qにより調製後，直ちに使用した．

**2. 試験標準溶液** ヘパリンナトリウムを水に溶解し，ヘパリンナトリウム標準溶液（20 mg/ml）とした．また，OSCS及びDSは水に溶解し，それぞれOSCS標準溶液（4 mg/ml）及びDS標準溶液（4 mg/ml）を調製した．各試験ではこれらの標準溶液を用い，分析能パラメーター評価用試験溶液の濃度に調整後試験に用いた．なお，これらの標準溶液はあらかじめポアサイズ0.45 μmの酢酸セルロース製メンブランフィルターによりろ過した後，試験に供した．

**3. 分析条件** キャピラリー電気泳動装置としてBeckman P/ACE MDQ Glycoprotein Systemを用いた．キャピラリーカラムは0.1 M水酸化ナトリウムで10分間，続いて10分間水で洗浄し，3回の空試験を行った後に試験に使用した．キャピラリーカラムは分析毎に，水で4分間，泳動用緩衝液で4分間洗浄した．

1) FDA method：キャピラリーカラムはフューズドシリカキャピラリー（GL Sciences社製，内径50 μm，有効長56 cm）を用いた．電気泳動用緩衝液［36 mM Sodium phosphate buffer (pH3.5)］は，リン酸二水素一ナトリウム一水和物1.0 gを水195 mlに溶解し，リン酸でpHを3.5に調整した後，水を加えて200 mlとし，ポアサイズ0.45 μmの酢酸セルロース製メンブランフィルターでろ過後，脱気して用いた．検出は，紫外部吸収検出（200 nm）により行った．印加電圧は30 kVで，試料導入側を陰極，廃液側を陽極として電気泳動した．分析温度は25℃とした．試料は加圧法（0.7 psi）により30秒間導入した．

2) OSCS method：キャピラリーカラムはフューズドシリカキャピラリー（GL Sciences社製，内径25 μm，有効長20 cm）を用いた．電気泳動用緩衝液［1000 mM Tris-phosphate buffer (pH3.5)］は，トリス30 gを水200 mlに溶解し，リン酸でpHを3.5に調整した後，水を加えて250 mlとし，ポアサイズ0.45 μmの酢酸セルロース製メンブランフィルターでろ過後，脱気して用いた．検出は紫外部吸収検出（200 nm）により行った．電流値を50 μAに設定し，試料導入側を陰極，廃液側を陽極として電気泳動した．分析温度は25℃とした．試料注入は加圧法（3.0 psi）により30秒間導入した．

3) DS method：キャピラリーカラムはフューズドシリカキャピラリー（GL Sciences社製，内径50 μm，有効長20 cm）を用いた．電気泳動用緩衝液［100 mM Tris-phosphate buffer (pH2.5)］は，トリス3.0 gを水200 mlに溶解し，リン酸でpHを2.5に調整した後，水を加えて250 mlとし，ポアサイズ0.45 μmの酢酸セルロース製メンブランフィルターでろ過後，脱気して用いた．検出は紫外部吸収検出（200 nm）により行った．電流値を80 μAに設定し，試料導入側を陰極，廃液側を陽極として電気泳動した．分析温度は25℃とした．試料注入は加圧法（0.7 psi）により30秒間導入した．

**4. 分析能パラメーターの評価** キャピラリー電気泳動装置としてBeckman P/ACE MDQ Glycoprotein Systemを用いて試験を実施し，Beckman 32 Karat Gold Software Version 7.0を用いてピーク面積値を算出した．ピーク面積値は最小ピーク幅設定値を2秒とし，OSCS及びDSのピーク開始点とピーク終了点を結ぶ傾斜線をベースラインとして検出されるピークの積算値から求めた．

**4-1. OSCS** ヘパリンナトリウム標準溶液 (20 mg/ml) 0.8 ml に，OSCS 標準溶液 (4 mg/ml) をそれぞれ 0.004, 0.01, 0.02, 0.04, 0.2 及び 0.4 ml を添加し，ついで水を 0.796, 0.79, 0.78, 0.76, 0.6 及び 0.4 ml 加えて混和し，ヘパリンナトリウムに対して OSCS がそれぞれ 0.1, 0.25, 0.5, 1.0, 5.0 及び 10.0% (w/w) 含む溶液とした．これらの溶液を分析能パラメーター評価用試験溶液とし，キャピラリー電気泳動装置を用いて測定した．

真度，併行精度及び室内再現精度は，5.0% OSCS を含むヘパリンナトリウム試験溶液を用いて各 6 回分析を行い，OSCS のピーク面積値を用いて算出した．特異性は 10% OSCS を含むヘパリンナトリウム試験溶液を用いて求めた．検出限界及び定量限界は 0.1–5.0% の OSCS を含むヘパリンナトリウム試験溶液を，直線性及び範囲は 0.1–10.0% の OSCS を含むヘパリンナトリウム試験溶液を用いて求めた．

**4-2. DS** ヘパリンナトリウム標準溶液 (20 mg/ml) 0.4 ml に，DS 標準溶液 (4 mg/ml) をそれぞれ 0.005, 0.01, 0.02, 0.05, 0.1 及び 0.2 ml を添加し，ついで水を 0.395, 0.39, 0.38, 0.35, 0.3 及び 0.2 ml 加えて混和し，ヘパリンナトリウムに対して DS がそれぞれ 0.25, 0.5, 1.0, 2.5, 5.0 及び 10.0% (w/w) 含む溶液とした．これらの溶液を分析能パラメーター評価用試験溶液とし，キャピラリー電気泳動装置を用いて測定した．

真度，併行精度及び室内再現精度は，5.0% DS を含むヘパリンナトリウム試験溶液を用いて各 6 回分析を行い，DS のピーク面積値を用いて算出した．特異性は 5.0% DS を含むヘパリンナトリウム試験溶液を用いて求めた．検出限界及び定量限界は 0.25–5.0% の DS を含むヘパリンナトリウム試験溶液を，直線性及び範囲は 0.25–10.0% の DS を含むヘパリンナトリウム試験溶液を用いて求めた．

## 結　　果

### 1. OSCS

**1-1. OSCS の分析条件** FDA がホームページ上に公開したキャピラリー電気泳動法による OSCS のスクリーニング方法 (FDA method) を参考にして，[8] 10% (w/w) の濃度で OSCS を添加したヘパリンナトリウム溶液を分析した．その結果，ヘパリンナトリウムに由来するピークは 5.8 分に泳動され，OSCS に由来するピークは 5.5 分に観察された [Fig. 2(a)]．両者を識別することは可能であったが，ヘパリンナトリウム由来のピークと OSCS 由来のピークの分離は不完全であり，OSCS 検出に対する特異性は低かった．したがって，FDA method を用いる試験法の分析能パラメーターは，真度 (添加回収率) が 41% (R.S.D.＝2.18%) であった．検出限界は 1.5% であり，$^1$H-NMR による OSCS 分析の分析能パラメーターと比べ低い値を示した (Table 1)．[12,13] なお，FDA method の併行精度は 1.36 %となり，室内再現精度は 2.17% となったことから，ヘパリンナトリウムと OSCS の分離を改善できれば，日本薬局方の純度試験として十分に採用できると考えられた．そこで，ヘパリンナトリウムと OSCS の分離の向上を目指し分析条件を検討した．

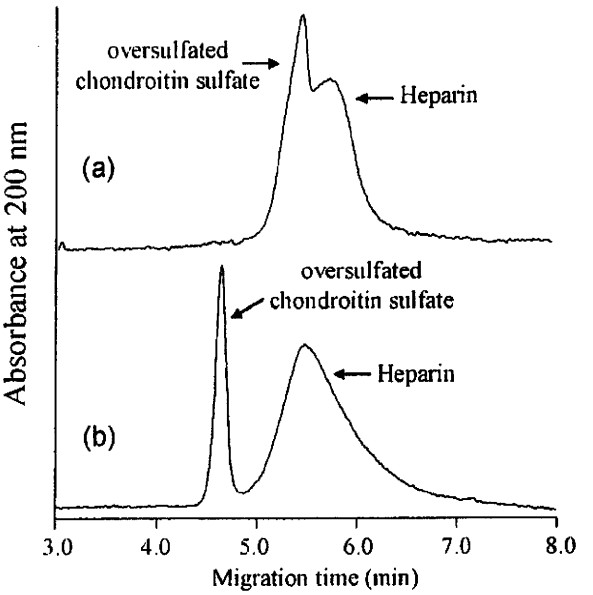


Fig. 2. Capillary Electrophoresis Analysis of 10% (w/w) OSCS Spiked Heparin
(a) FDA method and (b) OSCS method.

最近，Somsen らや Wielgos らは，ヘパリンナトリウムと OSCS の分離の改善例として，高い塩濃度の泳動緩衝液を用いる方法を紹介しており，高濃度緩衝液中では試料イオンがスタッキング効果により濃縮され，ピーク幅が縮小するためヘパリンナトリウムと OSCS の分離が向上することを報告している．[14,15] 一方，緩衝液中の塩濃度が高くなると，泳動時の電流値が高値になり分析が安定せず，発熱

Table 1. Validation Characteristics for OSCS Analysis by Capillary Electrophoresis and $^1$H-NMR

| Validation characteristics | Capillary electrophoresis | | $^1$H-NMR*2 |
|---|---|---|---|
| | OSCS method | FDA method*1 | |
| Accuracy | 93.7% (R.S.D.=3.83%) | 41% (R.S.D.=2.18%) | 98.3% (R.S.D.=4.63%) |
| Precision | | | |
| Repeatability | 2.11% | 1.36% | 1.6% |
| Intermed. precision | 2.45% | 2.17% | — |
| Specificity | Fig. 2b | | High |
| Detection limit | 0.1% (w/w) | 1.5% (w/w) | 0.35% (w/w) |
| Quantification limit | 0.25% (w/w) | 1.5% (w/w) | 0.4% (w/w) |
| Linearity | y=16992x+3601.6 ($R^2$=0.9996) | y=36663x−367.14 ($R^2$=0.9758) | y=0.0909x−0.064 ($R^2$=0.9991) |
| Range | 0.1–10.0% (w/w) | 1.5–10.0% (w/w) | 0.4–10.0% (w/w) |

*1 and *2, from the reports by Hashii *et al.*[12] and Kakehi *et al.*[13] respectively.

により安定した電気泳動が困難となる．これらの問題を解決するために，キャピラリーの内径を 50 μm から 25 μm に変更して電気泳動中に流れる電流量を抑制し，さらに用いる塩を比較的電気伝導度が低いトリスに変更することで電流値を抑制した．本条件では，高濃度塩，低 pH の緩衝液を使用するため，緩衝能の低下の恐れがあるが，繰り返し分析でも高い再現性を与え分析上問題はなかった（data not shown）．加えて，安定に電気泳動するために定電流モード（50 μA）で泳動することとした．また検出に関しては，ヘパリンナトリウムはアセチル基の含有率が低いため紫外部吸収では高い感度を示さないことが知られている．しかし，200 nm の紫外部吸収で検討したところ，ヘパリンナトリウムはオンカラム検出により特に問題はなく検出できた．さらにアセチル基を有する OSCS や DS などの不純物を高感度で検出できるため，純度試験として十分適用できる．以上のことから，本試験では 200 nm の紫外部検出を用いることとした．

以上の検討により設定した条件（OSCS method）を用いて，OSCS を 10%（w/w）添加したヘパリンナトリウム溶液を分析した．その結果，ヘパリンナトリウムに由来するピークは 5.5 分に観察され，OSCS に由来するピークは 4.6 分に観察された［Fig. 2(b)］．FDA method により測定した結果［Fig. 2(a)］と比較すると，ヘパリンナトリウムと OSCS の分離が格段に向上した．分離が向上した要因として，Somsen らや Wielgos らが報告した高濃度緩衝液中での試料イオンのスタッキング効果や，[14,15] 泳動緩衝液に用いたトリスが，カウンターイオンとして試料イオンと良好な相互作用を示したことなどが考えられる．また，キャピラリーの有効長を 20 cm に短縮しても十分な分離を達成でき，Somsen らの報告の半分の時間で分析が完了した．[14]

**1-2. OSCS 試験の分析法バリデーション**　前項において設定した OSCS method を用いて，日本薬局方医薬品各条ヘパリンナトリウム純度試験への適用を検討した．分析法バリデーションは，日本薬局方「参考情報」に記載されている方法にしたがい，7 つの分析能パラメーター（真度，精度，特異性，検出限界，定量限界，直線性，範囲）を求めることで試験法の妥当性を評価した．

**1-2-1. 特異性**　OSCS を 10%（w/w）添加したヘパリンナトリウム溶液を試験溶液として測定した結果，ヘパリンナトリウムに由来するピークは 5.5 分をピーク頂点とし 5.0–7.0 分に泳動され，OSCS に由来するピークが 4.6 分をピーク頂点として泳動された［Fig. 2(b)］．ヘパリンナトリウム由来のピークと OSCS 由来のピークは良好な分離を示し（分離度 Rs=1.2），両者を容易に識別できた．

**1-2-2. 検出限界及び定量限界**　0.1–5.0%（w/w）になるように OSCS の濃度を調製したヘパリンナトリウム試験溶液を用いて，OSCS method の検出限界及び定量限界を求めた．その結果，Fig. 3 に示すように 0.1% の OSCS を含む試験溶液でも，S/N 比 5 以上の感度で OSCS 由来のピークを検出できた．よって OSCS method は，ヘパリンナトリウ

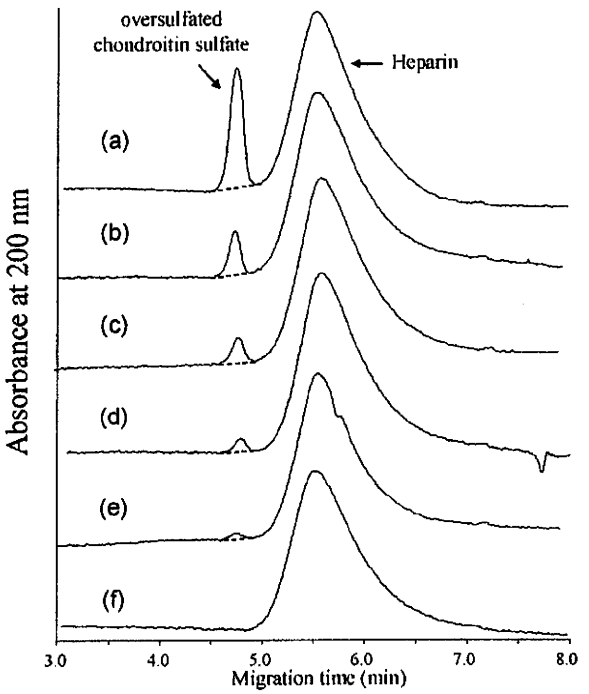


Fig. 3. Lower Limit of Detection of OSCS in the Presence of Heparin

Samples were analyzed at (a) 5.0%, (b) 1.0%, (c) 0.5%, (d) 0.25%, (e) 0.1% and (f) 0% OSCS spiked heparin. OSCS method was used for all analyses.

ム中に混入した0.1% (w/w) のOSCSを検出できる試験法であることがわかった．また，ヘパリンナトリウム中の0.25% (w/w) のOSCSを含む試験溶液において，OSCS由来のピークをS/N比10以上の感度で検出できたため，本試験法の定量限界とした．

**1-2-3. 直線性，範囲**　0.1–10.0% (w/w) になるようにOSCSの濃度を調整したヘパリンナトリウム試験溶液を用いて，OSCS methodの直線性を評価した．その結果，OSCSのピーク面積値は，0.1–10.0% (w/w) の範囲で優れた直線性が確認され，その相関係数は0.9996であった (Table 1)．

**1-2-4. 真度及び精度**　5.0% (w/w) のOSCSを含むヘパリンナトリウム試験溶液を用いて，添加回収実験を行いOSCS methodにおける真度を評価した．その結果，添加回収率は93.7% (R.S.D.＝3.83%) であった．FDA methodでの真度は，41% (R.S.D.＝2.18%) であったことから (Table 1)，著しい回収率の向上がみられた．よってOSCS methodは高い真度を有する試験法であると言える．

また，同じ試験溶液を用いてOSCS methodの精度の評価を行った．OSCSピーク面積値の併行精度 (1試験日，6回測定) のR.S.D.は2.11%であった．一方，室内再現精度 (3試験日，各6回測定) のR.S.D.は2.45%であった (Table 1)．併行精度並びに室内再現精度ともに，優れたR.S.D.値を示した．

**2. DS**

**2-1. DSの分析条件**　前節で設定したOSCS methodを用いて，5.0% (w/w) のDSを添加したヘパリンナトリウム溶液を分析したところ，DSに由来するピークは，6.4分をピーク頂点とし，6.0–7.0分にかけてブロードなピークとして観察された [Fig. 4(a)]．DS由来のピークは広がって観察されるため，検出限界は1.0% (w/w) と$^1$H-NMRによる試験法や，FDA methodを用いるキャピラリー電気泳動法による試験法と比べても，十分な感度を有する試験法とは言えず (Table 2)，OSCS検出を目的に最適化したキャピラリー電気泳動法の条件では，DSを高感度に検出することは難しい．

そこで，泳動緩衝液のpHについて検討したところ，pH2.5の緩衝液を用いることにより，DS由来のピークを高い理論段数 (N＝1190) で観察することができ，OSCS methodの結果 (N＝470) と比較して良好な分離能を示した．以上の検討により設定したDS methodにより，DSを5.0% (w/w) の濃度で添加したヘパリンナトリウム溶液を分析した結果，DSは4.4分をピーク頂点とした，シャープなピークとして観察され，3.2分に観察されたヘパリンナトリウムのピークと良好に分離された [Fig. 4(b)]．

**2-2. DS試験の分析法バリデーション**

**2-2-1. 特異性**　DSを5.0% (w/w) 添加したヘパリンナトリウム溶液を試験溶液として測定した結果，ヘパリンナトリウムに由来するピークは3.2分をピーク頂点とし2.7–4.3分に泳動され，DSに由来するピークが4.4分をピーク頂点として泳動された [Fig. 4(b)]．ヘパリンナトリウム由来のピークとDS由来のピークは良好な分離を示し (分離度Rs＝1.3)，両者を容易に識別できた．

**2-2-2. 検出限界及び定量限界**　0.25–5.0% (w/w) になるようにDSを添加したヘパリンナトリウム試験溶液を用いて，DS methodの検出限界及

び定量限界を確認した．その結果，Fig. 5 に示すように 0.25% の DS を含むヘパリンナトリウム試験溶液において S/N 比 5 以上の感度で DS 由来のピークを検出できた．また，ヘパリンナトリウム中の 0.5% (w/w) の DS を含む試験溶液において，DS 由来のピークを S/N 比 10 以上の感度で検出できたため，本試験法の定量限界とした．

**2-2-3. 直線性，範囲** 0.25–10.0% (w/w) になるように DS を添加したヘパリンナトリウム試験溶液を用いて，DS method の直線性を評価した．その結果，DS のピーク面積は，0.25–10.0% (w/w) の範囲で優れた直線性が確認され，その相関係数は 0.9998 であった (Table 2)．

**2-2-4. 真度及び精度** 5.0% (w/w) の濃度になるように DS を添加したヘパリンナトリウム試験溶液を用いて，添加回収実験により真度を評価した．その結果，添加回収率は 88.1% (R.S.D.＝2.13

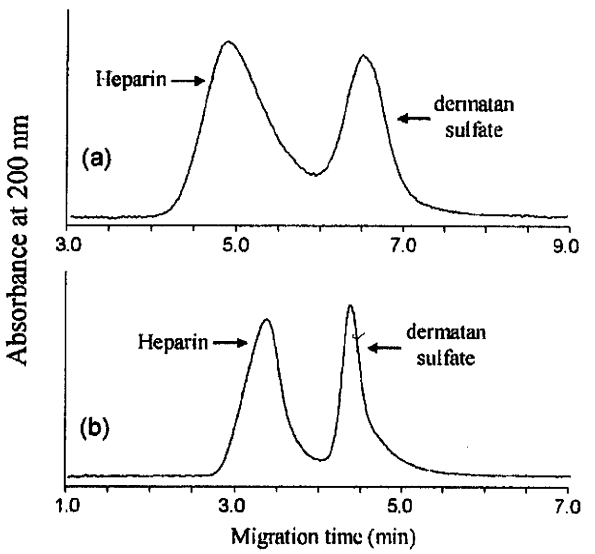


Fig. 4. Capillary Electrophoresis Analysis of 5.0% (w/w) DS Spiked Heparin
(a) OSCS method and (b) DS method.

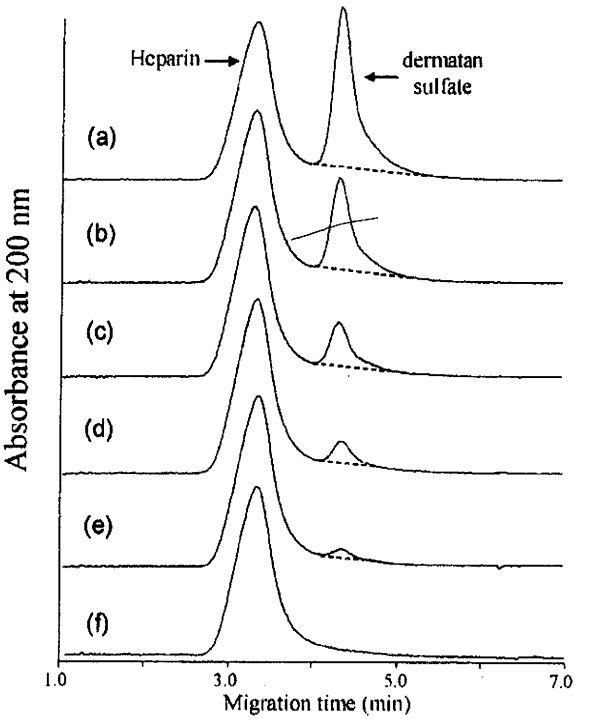


Fig. 5. Lower Limit of Detection of DS in the Presence of Heparin
Samples were analyzed at (a) 5.0%, (b) 2.5%, (c) 1.0%, (d) 0.5%, (e) 0.25% and (f) 0% DS spiked heparin. DS method was used for all analyses.

Table 2. Validation Characteristics for DS Analysis by Capillary Electrophoresis and $^1$H-NMR

| Validation characteristics | Capillary electrophoresis | | $^1$H-NMR*2 |
|---|---|---|---|
| | DS method | FDA method*1 | |
| Accuracy | 88.1% (R.S.D.＝2.13%) | 82% (R.S.D.＝1.78%) | 102.6% (R.S.D.＝3.99%) |
| Precision | | | |
| Repeatability | 1.99% | 2.15% | 1.5% |
| Intermed. precision | 2.43% | 2.48% | — |
| Specificity | Fig. 4b | | fair |
| Detection limit | 0.25% (w/w) | 1.0% (w/w) | 0.35% (w/w) |
| Quantification limit | 0.5% (w/w) | 1.0% (w/w) | 0.6% (w/w) |
| Linearity | y＝135944x－2904.9 ($R^2$＝0.9998) | y＝16938x－9357.2 ($R^2$＝0.9991) | y＝0.08534x－0.0113 ($R^2$＝0.9991) |
| Range | 0.25–10.0% (w/w) | 1.0–10.0% (w/w) | 0.6–18.7% (w/w) |

*1 and *2, from the reports by Hashii *et al.*[12] and Kakehi *et al.*[13] respectively.

%）であった．

また，同じ試験溶液を用いて精度の評価を行った．DSピーク面積値の併行精度（1試験日，6回測定）のR.S.D.は1.99%であった．一方，室内再現精度（3試験日，各6回測定）のR.S.D.は2.43%であった．併行精度並びに室内再現精度ともに，優れたR.S.D.値を示した．

**3. 有害ロットのヘパリンナトリウム製剤原料の分析**　前節までに検討した3種類の条件で，実際に有害事象を引き起こしたヘパリンナトリウム製剤原料の分析を行った．FDA methodでは，6.2分にヘパリンナトリウムのピークが，6.0分にOSCSのピークが観察された［Fig. 6(a)］．両者の識別は可能であったが分離は不十分であった．次に，OSCS methodにて分析した結果，ヘパリンナトリウムのピークは5.7分付近に，OSCSのピークは4.3分付近に観察され良好な分離を示した［Fig. 6(b)］．また，DS methodで分析した結果，ヘパリンナトリウムのピークは3.2分付近に，OSCSのピークは2.6分付近に観察された［Fig. 6(c)］．このヘパリンナトリウム製剤原料中にOSCSが8.6% (w/w)混入していると算出された．一方，本製剤原料中にはDS由来のピークは観察されなかった．

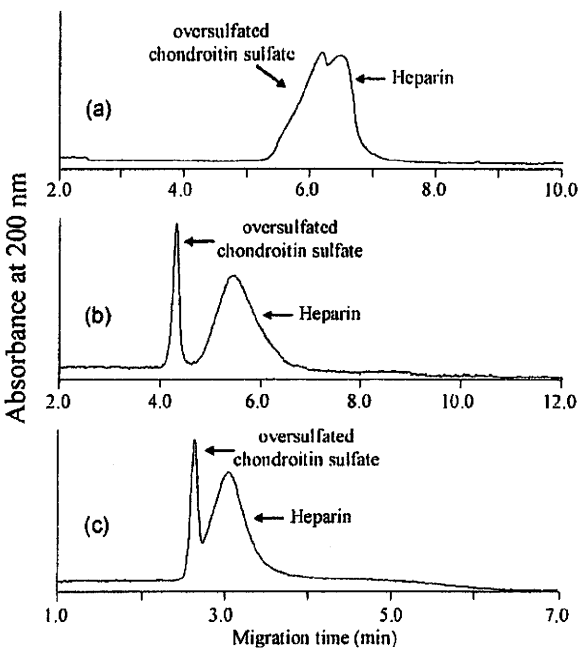


Fig. 6. Capillary Electrophoresis Analysis of Contaminated Heparin Sodium Preparation
(a) FDA method, (b) OSCS method and (c) DS method.

## 考　　察

**1. OSCS**　キャピラリー電気泳動法を日本薬局方医薬品各条ヘパリンナトリウム純度試験に用いるためには，OSCSを特異的に検出できる分析条件を設定する必要がある．高濃度の塩を含有する泳動緩衝液（1000 mM Tris-phosphate buffer）を用いる条件を検討し（OSCS method），ヘパリンナトリウムとOSCSを良好に分離できた（Fig. 2）．さらにOSCS methodは，キャピラリーの有効長を短縮しても十分な分離を達成できたことから，これまでに報告されたキャピラリー電気泳動法によるOSCS検出や，[14] Trehyらの報告した陰イオン交換カラムを用いるHPLC法によるOSCS検出と比べても，[9] 高いスループットを備えた分析法といえる．

本分析法はOSCS検出に対して高い特異性を有し［Fig. 2(b)］，ヘパリンナトリウム中に混入した0.1% (w/w)のOSCSを検出できた（Fig. 3）．また，真度（添加回収率：93.7%）や併行精度（R.S.D.=2.11%），室内再現精度（R.S.D.=2.45%）も良好であり，優れた直線性（$R^2$=0.9996）を示した（Table 1）．これらの結果から，OSCS methodは，ヘパリンナトリウム中のOSCS含量が0.1% (w/w)以下であることを保証する限度試験として，日本薬局方医薬品各条ヘパリンナトリウム純度試験に適用できる試験法であると判断される．

OSCSは今回の有害事象の原因物質であり，また製造工程由来物質や目的物質関連物質として混入する可能性がないことから，ヘパリンナトリウム製剤中に検出されるべきではない．したがって，ヘパリンナトリウム中に混入したOSCSの検出感度ができる限り高い試験法を用いることが望ましい．今回の事件を受けて，日本薬局方に規定された$^1$H-NMRによるOSCS試験の検出限界は0.35% (w/w)である．[12] OSCS methodによるキャピラリー電気泳動法は，$^1$H-NMRによる試験法を上回る検出感度を有している．そのため，キャピラリー電気泳動法によるOSCS試験は日本薬局方各条純度試験として有用であると評価できる．

**2. DS**　OSCS methodでは，DS由来のピークがブロードに観察されることから，ヘパリンナトリウム中の微量のDSを高い特異性で検出することが難しい［Fig. 4(a)］．そこでDSの感度向上を目

的とした条件(DS method)を検討した．その結果，DSとヘパリンナトリウムを良好に分離でき，併行精度（R.S.D.＝1.99%），室内再現精度（R.S.D.＝2.45%），真度（添加回収率：88.1%）を与える分析条件を設定することができた（Table 2）．DS methodは0.25—10.0%（w/w）の範囲で高い直線性（$R^2$=0.9998）が確認されたことから，DS検出に高い特異性と定量性を有した試験法であることがわかった．以上の結果から，キャピラリー電気泳動法によるDS分析は，ヘパリンナトリウム中のDSの混入が0.25%以下であることを保証する限度試験として日本薬局方の純度試験法に採用可能であると判断される．

今回の問題を受けて，米国薬局方に規定された$^1$H-NMRによる試験法では，500 MHzの装置を用いている．この際のDSの検出限界は0.35%である．一方で，国内の多くの製薬企業が設置している400 MHz以下のNMR装置を用いるDS試験では，特異性や検出限界などに問題が残されている．[12] よって，DSに関して高い特異性と検出限界を有するキャピラリー電気泳動法は有用な試験法であり，日本薬局方医薬品各条ヘパリンナトリウム純度試験に適した試験法と言える．

現在，臨床で使用されているヘパリン関連製剤や，同じグリコサミノグリカン類を原料とするヒアルロン酸製剤中に，一定量のDSが混入しているという報告がみられる．[16,17] そのため製剤中へのDS混入の規制の必要性については，DSはヘパリンとは異なる物質であるので，純度試験として適切に規制するべきとする意見と，これまでに毒性等の報告がなく純度試験等により規制する必要はないとする意見があり，国際的にも見解が分かれている．DSはヘパリンを調製する際の原料に含まれるため，ヘパリンの精製の指標として有用であるとも考えられ，今後は国内ヘパリンナトリウム中へのDSの含有量の実態を正確に把握した上で，規制が必要か否か検討していく必要があろう．

## 結　　論

本研究における分析法バリデーションの結果，キャピラリー電気泳動法は日本薬局方各条ヘパリンナトリウム純度試験として適用可能であることがわかった．

今後は他機関と連携した共同検定を行い，その他の規格を設定していく必要がある．特に検出限界に関しては，他機関においても同程度の値を得るため，分析試料の濃度や試料導入法，試料導入量などを規定しなければならない．

**謝辞**　ヘパリンナトリウム製剤原料をご供与いただきました日本バルク薬品㈱に深く御礼申し上げます．

## REFERENCES

1) Petitou M., Casu B., Lindahl U., *Biochimie*, **85**, 83–89 (2003).
2) Fischer K. G., *Hemodial. Int.*, **11**, 178–189 (2007).
3) Hirsh J., Levine M. N., *Blood*, **79**, 1–17 (1992).
4) Kishimoto T. K., Viswanathan K., Ganguly T., Elankumaran S., Smith S., Pelzer K., Lansing J. C., Sriranganathan N., Zhao G., Galcheva-Gargova Z., Al-Hakim A., Bailey G. S., Fraser B., Roy S., Rogers-Cotrone T., Buhse L., Whary M., Fox J., Nasr M., Dal Pan G. J., Shriver Z., Langer R. S., Venkataraman G., Austen K. F., Woodcock J., Sasisekharan R., *N. Engl. J. Med.*, **358**, 2457–2467 (2008).
5) ⟨http://www.fda.gov/cder/drug/infopage/heparin/adverse_events.htm.⟩, 6 June, 2009
6) Guerrini M., Beccati D., Shriver Z., Naggi A., Viswanathan K., Bisio A., Capila I., Lansing J. C., Guglieri S., Fraser B., Al-Hakim A., Gunay N. S., Zhang Z., Robinson L., Buhse L., Nasr M., Woodcock J., Langer R., Venkataraman G., Linhardt R. J., Casu B., Torri G., Sasisekharan R., *Nat. Biotechnol.*, **26**, 669–675 (2008).
7) ⟨http://www.fda.gov/cder/drug/infopage/heparin/heparin_NM_method.pdf.⟩, 6 June, 2009.
8) ⟨http://www.fda.gov/cder/drug/infopage/heparin/heparin_CE_method.pdf.⟩, 6 June, 2009.
9) Trehy M. L., Reepmeyer J. C., Kolinski R. E., Westenberger B. J., Buhse L. F., *J. Pharm. Biomed. Anal.*, **49**, 670–673 (2009).
10) Volpi N., Maccari F., Linhardt R. J., *Anal.*

*Biochem.*, **388**, 140–145 (2009).

11) Tami C., Puig M., Reepmeyer J. C., Ye H., D'Avignon D. A., Buhse L., Verthelyi D., *Biomaterials*, **29**, 4808–4814 (2008).

12) Hashii N., Kawasaki N., Takakura D., Itoh S., Kawahara N., Shoda T., Sugimoto N., Haishima Y., Shinagawa M., Shimba N., Miyata K., Tsukamoto H., Senshu K., Hasegawa T., Kawai K., Yoden H., Kinoshita M., Kakehi K., Goda Y., Okuda H., Tanamoto K., Yamaguchi T., *Pharm. Regul. Sci.*, **39**, 651–659 (2008).

13) Kakehi K., Kakoi N., Kinoshita M., Hashii N., Kawasaki N., Terao T., Kawai K., Yoden H., Yamaguchi T., *Pharm. Regul. Sci.*, **39**, 713–720 (2008).

14) Somsen G. W., Tak Y. H., Torano J. S., Jongen P. M., de Jong G. J., *J. Chromatogr. A.*, **1216**, 4107–4112 (2009).

15) Wielgos T., Havel K., Ivanova N., Weinberger R., *J. Pharm. Biomed. Anal.*, **49**, 319–326 (2009).

16) Neville G. A., Mori F., Holme K. R., Perlin A. S., *J. Pharm. Sci.*, **78**, 101–104 (1989).

17) Matsuno Y. K., Kakoi N., Kinoshita M., Matsuzaki Y., Kumada J., Kakehi K., *Electrophoresis*, **29**, 3628–3635 (2008).

Analytical Biochemistry 396 (2010) 161–163

Contents lists available at ScienceDirect

Analytical Biochemistry

journal homepage: www.elsevier.com/locate/yabio

Notes & Tips

# Determination of Tn antigen released from cultured cancer cells by capillary electrophoresis

Keita Yamada [a], Sakie Watanabe [a], Soichiro Kita [a], Mitsuhiro Kinoshita [a], Takao Hayakawa [b], Kazuaki Kakehi [a,*]

[a] School of Pharmacy, Kinki University, Kowakae 3-4-1, Higashi-Osaka 577-8502, Japan
[b] Pharmaceutical Research and Technology Institute, Kinki University, Kowakae 3-4-1, Higashi-Osaka 577-8502, Japan

ARTICLE INFO

*Article history:*
Received 27 July 2009
Available online 21 August 2009

ABSTRACT

An incomplete elongation of *O*-glycans in mucins has been found in epithelial cancers, leading to the expression of shorter carbohydrate structures such as Tn antigen (GalNAc-O-Ser/Thr), which has been reported to be one of the most specific human cancer-associated structures. However, there have been no appropriate physicochemical methods for the determination of Tn antigen in biological samples. In the present paper, we developed a capillary electrophoresis method for the determination of Tn antigen, and applied the method to the analysis of the expressed Tn antigen on some leukemia and epithelial cancer cells.



Cancer-associated structural alterations in *O*-glycans such as high level sialylation and low-level sulfation are attracting interest in relation to their biological significance [1]. Especially, incomplete elongation of *O*-glycans in mucins has been found in many cancers, leading to the expression of shorter carbohydrate structures, such as Tn antigen (GalNAc-O-Ser/Thr) [2], which is one of the most specific human cancer-associated structures and a possible early biomarker of cancer [3].

Current analytical methods for characterization of *O*-glycans involve the initial release of the oligosaccharides. However, the release of *O*-glycans has been a difficult task due to lack of the enzyme which shows wide specificity as in the case of *N*-glycoamidase for the release of *N*-glycans. Therefore, *O*-glycans still have to be released from the core proteins by chemical methods, and most of the methods require a lengthy reaction time and cumbersome procedures [4]. Recently, we developed an automated glycan-releasing apparatus (Autoglycocutter: AGC)[1] for *O*-glycosylated proteins [5,6]. The apparatus enables the release of *O*-glycans having the intact reducing end within only 3 min, and was applied to the analysis of *O*-glycans from some leukemia and epithelial cancer cells [7].

The released glycans are often labeled with a fluorescent tag, although we have to remove the excess reagents and the accompanying materials [8–11]. The procedures hitherto reported are effective for purification of higher oligosaccharides. Monosaccharides such as Tn antigen released from the samples are often poorly recovered when the clean-up procedures for higher oligosaccharides are applied.

In the current study, we developed a clean-up method for collection of Tn antigen and the small glycans, and applied the method to the analysis of Tn antigen in some cancer cell lines.

We used human-derived cell lines: Jurkat (acute T cell leukemia), U937 (histiocytic lymphoma), K-562 (chronic myelogenous leukemia), HL-60 (acute promyelocytic leukemia), LS174T and HCT-15 (colorectal adenocarcinoma), BxPC3 (pancreatic adenocarcinoma), PANC1 (pancreatic carcinoma), and MKN7 and MKN45 (gastric adenocarcinoma).

A portion of the glycopeptide fractions obtained from each cancer cell line ($1.0 \times 10^7$ cells) was injected to the AGC apparatus [6,7], and the collected solution containing the released *O*-glycans was evaporated to dryness followed by labeling with 2-aminobenzoic acid (2-AA) as reported previously [7].

In our previous work using Sephadex LH-20 for clean-up of 2-AA-labeled glycans, we could not recover Tn antigen in good efficiency [7]. We examined several clean-up procedures for the analysis of the 2-AA-labeled GalNAc, and calculated the recovery of GalNAc (Table 1). Most of the reported methods using carbon graphite columns [8], nylon filters [9], polyamide resin (DPA-6S) [10], and acetone precipitation [11] are optimized for the glycans having high molecular masses and not appropriate for clean-up of simple mono and disaccharides. Therefore, we examined an HPLC method using octadecylsilica as the stationary phase. Although a long time (60 min) is required for collection of the fractions containing Tn antigen, we found that higher than 99% of the excess amount of 2-AA was removed and 2-AA-labeled GalNAc was recovered quantitatively.

* Corresponding author.
*E-mail address:* k_kakehi@phar.kindai.ac.jp (K. Kakehi).

[1] *Abbreviations used:* 2-AA, 2-aminobenzoic acid; AGC, Autoglycocutter; CAE, capillary affinity electrophoresis.

0003-2697/$ - see front matter © 2009 Elsevier Inc. All rights reserved.
doi:10.1016/j.ab.2009.08.021

**Table 1**
Efficiencies in purification of 2-AA-labeled GalNAc using previously reported methods.

| Method | Removal of the reagent (%) | Recovery of GalNAc-2-AA (%) | Run time (min) | Reference [Reference No.] |
|---|---|---|---|---|
| Sehadex LH-20 | – | – | 180 | J. Proteome Res. 8 (2009) 521–537 [7] |
| ENVI-carb column | 10 | 34 | 60 | Clin. Chem 44 (1998) 2422–2428 [8] |
| Nylon filter | 99 | 69 | 60 | Anal. Biochem. 373 (2008) 104–111 [9] |
| Polyamide resin (DPA-6S) | 96 | 78 | 60 | Anal. Biochem. 369 (2007) 202–209 [10] |
| Acetone precipitation | 5 | 54 | 30 | Anal. Biochem. 384 (2009) 263–273 [11] |
| COSMOSIL(R) 5C18-PAQ (ID 4.6 × 150 mm) | 99 | 99 | 60 | Present method |

In the analysis of Tn antigen, it is necessary to resolve it from other possible monosaccharides and the accompanying materials. In the present study, we employed capillary electrophoresis and achieved excellent resolution of GalNAc (see Supplemental Fig. 1). During the alkali-catalyzed release of glycans from core peptides using the AGC apparatus, epimerization of the glycans is a big problem. We evaluated the epimerization reaction of Tn antigen. After the solution of the standard GalNAc was passed through AGC, the mixture was labeled with 2-AA and analyzed by CE. A small amount of *N*-acetyl-D-talosamine (TalNAc) was observed, but the peak area was 4.2% of GalNAc (see Supplemental Fig. 2). These results indicate that the effect of epimerization during the releasing reaction is negligible.

We applied the method to the analysis of the expressed Tn antigen on Jurkat cells (Fig. 1). After a large peak of the reagent with some artifact peaks, the peak due to Tn antigen was observed at ca. 53 min. It should be noted that a Tn peak at 53 min accompanies some minor components. After collection of this peak, we analyzed it by CE and capillary affinity electrophoresis (CAE), and found that the peak showed the same migration time as that of GalNAc by CE (Fig. 1B). In addition, CAE using the buffer containing $VVAB_4$ lectin (*Vicia villosa* seed) at 10 μM concentration, which specifically recognizes GalNAc [12], clearly caused disappearance of the peak at 8.9 min. In contrast, the peak of 2-AA maltopentaose (internal standard) at 10.3 min was not changed. These results indicate that the peak observed at 8.9 min was due to Tn antigen.

Based on the methods described above, we analyzed the expression of Tn antigen on some cancer cell lines (Fig. 1C). All cancer cell lines examined in this study expressed significantly different amounts of Tn antigen. Of the examined leukemia cell lines, Jurkat cells express Tn antigen most abundantly. Because Jurkat cells lack a molecular chaperone (cosmc) which is necessary for expression of core 1 beta 3 galactosyl transferase activity [13], Jurkat cells cannot establish the core 1 structure, and the truncated *O*-glycan (i.e., Tn antigen) which is a precursor of core 1 type glycans is abundantly observed. Epithelial cancer cells other than HCT-15 cells expressed Tn antigen more abundantly than Jurkat cells. Especially, LS174T cells expressed about 10 times larger amounts of Tn antigen than other epithelial cancer cells. We reported that poorly differentiated pancreatic cancer cells (PANC1) showed simple *O*-glycan profiles, but moderately differentiated pancreatic cancer cells (BxPC3) showed relatively complex *O*-glycan profiles. In sharp contrast with these results, MKN45 cells (poorly differentiated species) and MKN7 cells

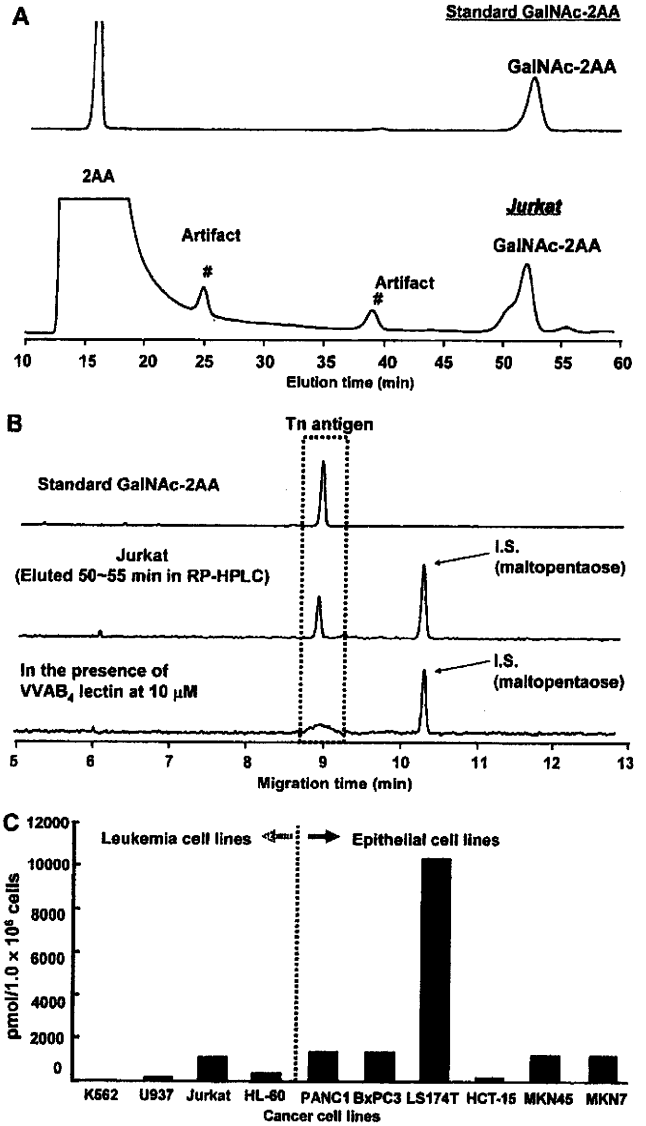


**Fig. 1.** Determination of Tn antigen in some cancer cells. Purification of 2-AA-labeled Tn antigen derived from Jurkat cells by RP-HPLC (A). Conditions for purification by RP-HPLC. Column, COSMOSIL 5C18-AR-II (4.6 × 150 mm); eluent, solvent A, 0.1% HCOOH in water; solvent B, 20% acetonitrile containing 0.1% HCOOH. Gradient elution; a linear gradient (10–20% solvent B) from 0 to 20 min, then followed by a linear gradient (20–22.5% solvent B) from 20 to 70 min. CE and CAE analysis of 2-AA-labeled Tn antigen form Jurkat cells (B). Analytical conditions for CE and CAE. Capillary, DB-1 capillary (100 μm i.d. × 40 cm); running buffer, 100 mM Tris–borate buffer (pH 8.3) containing 5% PEG70000; applied voltage, 25 kV; injection, pressure method (1.0 psi for 10 s); temperature, 25 °C; detection, helium–cadmium laser-induced fluorescence (excitation 325 nm, emission 405 nm). CAE of the Tn antigen from Jurkat cells in the presence of GalNAc-specific lectin ($VVAB_4$). The peak observed at 10.3 min was due to maltopentaose labeled with 2-AA, which is used as the internal standard for migration times. The migration time of 2-AA-labeled maltopentaose was not changed in the presence/absence of $VVAB_4$. Expression of Tn antigen in 10 cancer cell lines (C). The amount of Tn antigen was calculated by peak area observed by CE.

(well differentiated species) showed the reverse results [7]. Prior to starting this work, we had expected that expressions of Tn antigen are varied with stages of cancer differentiation. However, significant differences of the expression of Tn antigen were not observed in these four epithelial cancer cells. On the other hand, expression of Tn antigen was quite different between HCT-15 and LS174T, which are colon cancer cell lines. LS174T cells, high metastasis cells [14],

expressed the largest amount of Tn antigen of the examined cancer cells. However, HCT-15 cells, low metastasis cells [14], expressed trace amounts of Tn antigen. Hirao et al. indicated that Tn antigen could be used as a marker for the level of metastasis of uterine cervix cancer cells [15]. Our present results are well correlated with their observations.

In the present study, we developed a method for the analysis of Tn antigen, and found that high metastasis cancer cells expressed Tn antigen extremely abundantly. Although further studies using clinical samples are required, the present method will be a useful tool for characterization of clinical significance of cancer cells.

## Appendix A. Supplementary data

Supplementary data associated with this article can be found, in the online version, at doi:10.1016/j.ab.2009.08.021.

## References

[1] I. Brockhausen, Pathways of O-glycan biosynthesis in cancer cells, Biochim. Biophys. Acta 1473 (1999) 67–95.
[2] G.F. Springer, T and Tn, general carcinoma autoantigens, Science 224 (1984) 1198–1206.
[3] S.H. Itzkowitz, E.J. Bloom, T.S. Lau, Y.S. Kim, Mucin associated Tn and sialosyl-Tn antigen expression in colorectal polyps, Gut 33 (1992) 518–523.
[4] L. Royle, T.S. Mattu, E. Hart, J.I. Langridge, A.H. Merry, N. Murphy, D.J. Harvey, R.A. Dwek, P.M. Rudd, An analytical and structural database provides a strategy for sequencing O-glycans from microgram quantities of glycoproteins, Anal. Biochem. 304 (2002) 70–90.
[5] Y.K. Matsuno, K. Yamada, A. Tanabe, M. Kinoshita, S.Z. Maruyama, Y.S. Osaka, T. Masuko, K. Kakehi, Development of an apparatus for rapid release of oligosaccharides at the glycosaminoglycan–protein linkage region in chondroitin sulfate-type proteoglycans, Anal. Biochem. 362 (2007) 245–257.
[6] K. Yamada, S. Hyodo, Y.K. Matsuno, M. Kinoshita, S.Z. Maruyama, Y.S. Osaka, E. Casal, Y.C. Lee, K. Kakehi, Rapid and sensitive analysis of mucin-type glycans using an in-line flow glycan-releasing apparatus, Anal. Biochem. 371 (2007) 52–61.
[7] K. Yamada, M. Kinoshita, T. Hayakawa, S. Nakaya, K. Kakehi, Comparative studies on the structural features of O-glycans between leukemia and epithelial cell lines, J. Proteome Res. 8 (2009) 521–537.
[8] A. Klein, A. Lebreton, J. Lemoine, J.M. Perini, P. Roussel, J.C. Michalski, Identification of urinary oligosaccharides by matrix-assisted laser desorption ionization time-of-flight mass spectrometry, Clin. Chem. 44 (1998) 2422–2428.
[9] K.R. Anumula, Unique anthranilic acid chemistry facilitates profiling and characterization of Ser/Thr-linked sugar chains following hydrazinolysis, Anal. Biochem. 373 (2008) 104–111.
[10] B.D. Prater, K.R. Anumula, J.T. Hutchins, Automated sample preparation facilitated by PhyNexus MEA purification system for oligosaccharide mapping of glycoproteins, Anal. Biochem. 369 (2007) 202–209.
[11] M. Pabst, D. Kolarich, G. Poltl, T. Dalik, G. Lubec, A. Hofinger, F. Altmann, Comparison of fluorescent labels for oligosaccharides and introduction of a new postlabeling purification method, Anal. Biochem. 384 (2009) 263–273.
[12] G. Konska, M. Guerry, F. Caldefie-Chezet, M. De Latour, J. Guillot, Study of the expression of Tn antigen in different types of human breast cancer cells using VVA-B4 lectin, Oncol. Rep. 15 (2006) 305–310.
[13] T. Ju, R.D. Cummings, A unique molecular chaperone Cosmc required for activity of the mammalian core 1 beta 3-galactosyltransferase, Proc. Natl. Acad. Sci. USA 99 (2002) 16613–16618.
[14] D.L. Trainer, T. Kline, F.L. McCabe, L.F. Faucette, J. Feild, M. Chaikin, M. Anzano, D. Rieman, S. Hoffstein, D.J. Li, et al., Biological characterization and oncogene expression in human colorectal carcinoma cell lines, Int. J. Cancer 41 (1988) 287–296.
[15] T. Hirao, Y. Sakamoto, M. Kamada, S. Hamada, T. Aono, Tn antigen, a marker of potential for metastasis of uterine cervix cancer cells, Cancer 72 (1993) 154–159.

Analytical Biochemistry 388 (2009) 242–253

Contents lists available at ScienceDirect

Analytical Biochemistry

journal homepage: www.elsevier.com/locate/yabio

# Structural characterization of multibranched oligosaccharides from seal milk by a combination of off-line high-performance liquid chromatography–matrix-assisted laser desorption/ionization–time-of-flight mass spectrometry and sequential exoglycosidase digestion

Mitsuhiro Kinoshita [a], Hiroko Ohta [a], Kanata Higaki [a], Yoko Kojima [a], Tadasu Urashima [b], Kazuki Nakajima [c], Minoru Suzuki [c], Kit M. Kovacs [d], Christian Lydersen [d], Takao Hayakawa [e], Kazuaki Kakehi [a,*]

[a] Faculty of Pharmaceutical Sciences, Kinki University, Kowakae 3-4-1, Higashi-osaka 577-8502, Japan
[b] Graduate School of Food Hygine, Obihiro University of Agriculture and Veterinary Medicine, Obihiro-shi, Hokkaido 080-8555, Japan
[c] Sphingolipid Expression Laboratory; Supra-Biomolecular System Research Group, RIKEN Frontier Research System, Wako-shi, Saitama 351-0198, Japan
[d] Norwegian Polar Institute, N-9007 Tromsø, Norway
[e] Pharmaceutical Research and Technology Institute, Kinki University, Kowakae 3-4-1, Higashi-osaka 577-8502, Japan

ARTICLE INFO

*Article history:*
Received 4 December 2008
Available online 9 March 2009

*Keywords:*
Milk oligosaccharide
Multibranched polylactosamine-type oligosaccharide
MALDI–TOF MS
Exoglycosidase digestion
HPLC

ABSTRACT

A complex mixture of diverse oligosaccharides related to the carbohydrates in glycoconjugates involved in various biological events is found in animal milk/colostrum and has been challenging targets for separation and structural studies. In the current study, we isolated oligosaccharides having high molecular masses (MW ~ 3800) from the milk samples of bearded and hooded seals and analyzed their structures by off-line normal-phase–high-performance liquid chromatography–matrix-assisted laser desorption/ionization–time-of-flight (NP–HPLC–MALDI–TOF) mass spectrometry (MS) by combination with sequential exoglycosidase digestion. Initially, a mixture of oligosaccharides from the seal milk was reductively aminated with 2-aminobenzoic acid and analyzed by a combination of HPLC and MALDI–TOF MS. From MS data, these oligosaccharides contained different numbers of lactosamine units attached to the nonreducing lactose (Galβ1–4Glc) and fucose residue. The isolated oligosaccharides were sequentially digested with exoglycosidases and characterized by MALDI–TOF MS. The data revealed that oligosaccharides from both seal species were composed from lacto-*N*-neohexaose (LNnH, Galβ1–4GlcNAcβ1–6[Galβ1–4GlcNAcβ1–3]Galβ1–4Glc) as the common core structure, and most of them contained Fucα1–2 residues at the nonreducing ends. Furthermore, the oligosaccharides from both samples contained multibranched oligosaccharides having two Galβ1–4GlcNAc (*N*-acetyllactosamine, LacNAc) residues on the Galβ1–4GlcNAcβ1–3 branch or both branches of LNnH. Elongation of the chains was observed at 3-OH positions of Gal residues, but most of the internal Gal residues were also substituted with an *N*-acetyllactosamine at the 6-OH position.



Specific sequences of monosaccharides occur as important structural elements of oligo- and polysaccharides of glycoproteins and glycolipids, and they comprise recognition motifs for ligand–receptor or cell–cell interactions [1–4]. Oligosaccharides are cooperatively synthesized by actions of various glycosyltransferases and are usually present as a complex mixture of diverse oligosaccharides. In particular, the isomeric/branching structure is the major feature, and their structural determination is essential for understanding the biosynthesis and biological significance.

Mammalian milk/colostrum is a rich source of carbohydrates of diverse structures [5–8]. Although the most dominant carbohydrate in mammalian milk is generally lactose, a small amount of characteristic oligosaccharides are also present [9–13]. The milk oligosaccharides usually have a common lactose (Galβ1–4Glc) core that is extended at the 6- and/or 3-OH positions of the Gal as linear/branched mode [14]. Furthermore, the linear/branched chains are frequently fucosylated and/or sialylated and in a few cases are sulfated.

Due to the similarities and complex structures of milk oligosaccharides, structural determination of them has been a big and challenging work. Urashima and coworkers isolated various oligosaccharides from many mammalian species' milk/colostrum and characterized their structural features by a combination of

* Corresponding author. Fax: +81 6 6721 2353.
*E-mail address:* k_kakehi@phar.kindai.ac.jp (K. Kakehi).

0003-2697/$ - see front matter © 2009 Elsevier Inc. All rights reserved.
doi:10.1016/j.ab.2009.03.004